Small Molecule Potentiators of Oncolytic Virus Therapy Suppress the Innate Antiviral Response

Submitted by

Nader El-Sayes

A thesis submitted to the Faculty of Graduate and Postdoctoral Studies in partial fulfillment of the requirements for the degree of Master of Science, Specialization in Biochemistry

University of Ottawa

Faculty of Medicine

Department of Biochemistry, Microbiology, and Immunology

Supervisors:

Jean-Simon Diallo, PhD

Christopher Boddy, PhD

Abstract

Oncolytic Viruses (OVs) are often attenuated to increase their safety profile, however this can lead to reduced efficacy in heterogeneous malignancies and result in resistance to OV therapy. Our group utilizes small molecule enhancers of OV therapy termed viral sensitizers. These small molecules have been shown to enhance the replication and spread of oncolytic rhabdovirus VSVΔ51 *in vitro* and prolong survival in tumour-bearing mice. In this study, we evaluate the effect of these viral sensitizers on the innate antiviral response in order to identify the mechanism of action responsible for their viral-sensitizing properties. Our previous data suggest that VSe1 and its structural analogues affect the type I IFN antiviral response and have the potential to affect cellular redox homeostasis. We hypothesized that VSe1 and its structural analogues potentiate VSVΔ51 activity by inhibiting the type I IFN response via redox-mediated dysregulation. In this study, we demonstrate that the viral sensitizers inhibit the nuclear translocation and transcriptional activity of NFκB, which in turn dampens the expression of antiviral cytokines IFN-β, TNFα and IL-6. We also provide evidence supporting the possibility that the NFκB inhibition may be a result of the formation of ROS intermediates by the viral sensitizers, which leads to reduced nuclear translocation of NFκB subunits, thereby preventing NFκB-mediated cytokine production. Overall, this work contributes to the identification of the mechanism of action of our viral sensitizers and highlights the finding that oncolytic VSV infection can be enhanced through redox-mediated modulation of the innate antiviral response.

Acknowledgements

First and foremost, to Dr. Jean-Simon Diallo, thank you for your mentorship and guidance, and for the opportunity to learn and develop as a researcher in such a positive research environment. To Dr. Rozanne Arulanandam and Ramya Krishnan, thank you for your valuable ideas and suggestions, which were instrumental for the development of this project. To Johanne Mathieu, thank you for all the hard work you have put into this project. To Dr. Mary-Ellen Harper and David Patten, thank you for sharing your expertise and for helping with the HPLC experiments. To my fellow Diallo lab members Naveen, Nicole, Fanny, Mohsen, Andrew, Oliver, Connie, and Samriti, thank you for the friendly environment you have created. To Dr. Marie-Claude Bourgeois-Daigneault, Amelia Sadie Aitken, Sarwat Tahsin Khan, and Dylan Kassapa Siriwardena thank you for your friendship. You are by far some of the smartest and most enjoyable people I know. Lastly, to my parents Ahmad and Iman, and my sister Jenin, thank you for all your support. My past, present and future achievements are all attributed to the guidance you have provided all these years.

Table of Contents

List of Abbreviations

AP1	Activating protein 1	MAPK	mitogen-activated protein kinases
ATF2	Activating transcription factor 2	MDA5	melanoma differentiation-associated antigen 5
BSO	L-Buthionine-sulfoximine	MKK	MAPK kinase
CARD	caspase activation and recruitment domains	MOI	Multiplicity of infection
CBP	CREB-binding protein	MSK	mitogen- and stress-activated protein kinase
CREB	Cyclic-AMP-responsive-element-binding protein	MX2	MX dynamin like GTPase 2
DMSO	Dimethyl sulfoxide	MyD88	myeloid differentiation primary response gene 88
GRX	Glutaredoxin	NFκB	nuclear factor kappa–light-chain-enhancer of activated B
GSH	Reduced glutathione	NIK	NFκB-inducing kinase
GSSG	Oxidized glutathione	OSGIN	oxidative stress induced growth inhibitor
GST	Glutathione-S-transferase	OV	Oncolytic virus
GSTP1	GST pi 1	PAMP	pathogen-associated molecular patterns
H_2O_2	Hydrogen peroxide	PKA	Protein kinase A
HDAC	Histone deacetylase	PRR	Pathogen recognition receptor
HMOX-1	Heme oxygenase 1	RHD	Rel homology domain
HPLC	High-performance liquid chromatography	RIG-I	Retinoic acid-inducible gene
IFITM1	IFN-induced transmembrane protein 1	RLR	RIG-I-like receptors
IFN	Interferon	ROS	Reactive oxygen species
IFNAR	IFN α/β receptor	RSK	Ribosomal subunit kinase

IKK	IκB kinase	STAT	signal transducer and activator of transcription
IL-6	Interleukin 6	TBK1	Tank-binding kinase 1
IPS-1	IFN promoter stimulator 1	TK	Thymidine kinase
IRF	IFN regulatory factor	TLR	Toll-like receptor
ISG	IFN-stimulated gene	TNFR	TNF receptor
ISGF3	ISG factor 3	TNFα	Tumour necrosis factor α
ISRE	IFN-stimulated response element	TYK	Tyrosine kinase
IκB	inhibitor of NFκB	VSe	Viral sensitizer
JAK	Janus kinase	VSV	Vesicular stomatitis virus
JNK	c-jun N-terminal kinase	VSVΔ51	VSV M51 deletion
LDLR	Low-density lipoprotein receptor	VV	Vaccinia virus
LGP2	Laboratory of genetic and physiol-ogy 2	WT	Wild-type
MAF	musculoaponeurotic fibrosarcoma		

List of Figures

1. Introduction

1.1 Hallmarks of Cancer

Cancer is currently the leading cause of death in Canada, responsible for 30% of all deaths nationally. It is estimated that a staggering 50% of Canadians will develop cancer in their lifetime. In the year 2017 alone, 206 200 Canadians will develop cancer and 80 800 Canadians will die of cancer [1]. Cancer emergence relies on the rapid and uncontrolled proliferation of cells. This uncontrolled proliferation can be the result of genetic and/or epigenetic changes that have several causes including exposure to carcinogens, radiation or viral infection [2,3]. There are several hallmarks that collectively contribute to malignant growth: limitless replicative potential, self-sufficiency in growth signals, insensitivity to growth inhibitory signals, evasion of apoptosis, sustained angiogenesis, immune evasion, and tissue invasion and metastasis [4]. Chemotherapy coupled with surgical resection of the tumor mass is currently the most common treatment for cancer patients. Chemotherapeutics drugs are small molecules that exploit traits that are specific to cancer cells to selectively damage their cellular functions [5]. For example, alkylating agents capitalize on the rapid DNA replication of cancer cells [6], antimetabolites on their enhanced metabolism [7] and microtubule inhibitors on their hyperactive cell cycle and division [8]. While effective at killing cancer cells, chemotherapeutic agents can be subject to therapeutic resistance and are also not selective enough to entirely avoid damage to healthy cells, resulting in numerous and severe side effects such as nausea, vomiting, diarrhea, leukopenia and even sterility [5]. With the objective of maximizing therapeutic efficacy without significantly impacting patient quality of life, many alternative therapies are currently being investigated for cancer treatment. Indeed, biotherapies such as oncolytic virus (OV) therapy are emerging as promising alternatives to chemotherapy.

1.2 OVs

1.2.1 Mechanism of Action

OVs are a growing class of biotherapeutics that are engineered to selectively infect and kill cancer cells. The concept of OV therapy emerged from the early observation that viruses naturally have a preferential, though non-selective, tropism for cancer cells [9,10]. This cancer selectivity can be attributed to some of the hallmark changes in cancer cells (section 1.1) [4]. Indeed OVs can be engineered or selected to exploit several cancer properties such as high metabolic rates, defective programmed cell death pathways, and defective antiviral pathways [11]. Therefore cancer cells provide a unique niche for OVs to replicate, with minimal impact on normal tissues and only few transient side effects [11,12].

OVs are multimodal agents that induce cancer cell death through several mechanisms. The most direct mechanism responsible for OV-mediated cytotoxicity is the direct lysis of infected cells as a result of the natural life cycle of many viruses. Additionally, OVs can selectively infect the tumor vasculature, causing thrombosis which reduces blood flow to the tumour mass and leads to apoptosis and necrosis of cancer cells even in the absence of direct infection [13,14]. Furthermore, the combination of infection, apoptosis and necrosis of the OV-infected cells results in the secretion of many proinflammatory cytokines and chemokines that activate and attract immune cells to the tumor bed [15–18], which can overcome the immunosuppressive nature of the tumour microenvironment and lead to anti-tumor immune attack.

1.2.2 Selecting and Designing OV Candidates

As explained above, cancer cells are often highly susceptible to viral infection. While some naturally occurring viruses demonstrate selectivity towards malignant tissue, other viruses need to be genetically attenuated to increase their safety profile while maintaining the ability to infect

cancer cells. For example, a vaccinia virus (VV) variant was engineered to generate a safe OV by knocking out thymidine kinase (TK), an enzyme that catalyzes one of the steps in the synthesis of thymidine triphosphate. While TK is essential for VV to replicate efficiently in normal cells that express low levels of cellular TK, the rapid division of tumour cells provides a steady supply of nucleotides including thymidine triphosphate, therefore complementing the TK-/- virus [19]. Another example is the oncolytic Rhabdovirus Maraba MG1, a genetically engineered variant of Maraba virus with two mutations, identified through screening a series of attenuated mutations. Unlike the wild type (WT) variant of the virus, MG1 is impaired in its capacity to block interferon (IFN) production in response to infection, attenuating the capacity of the virus to infect healthy tissue while maintaining the capacity to infect malignant tissue [20].

Aside from improving the safety profile, several studies have focused on maximizing the extent of cancer-selective oncolysis to enhance the efficacy of OV therapies. For example, OVs have been engineered to express transgenes that inhibit cell proliferation [21], suicide genes [22], or fusion proteins that induce syncytium formation [23]. Oncolysis can also be enhanced using combinations of OVs with existing anticancer molecules such as Triptolide [24] and Paclitaxel [25].

1.2.3 Oncolytic VSV

Like Maraba virus, Vesicular stomatitis virus (VSV) is a single-stranded, negative-sense RNA virus of the family *Rhabdoviridae.* While VSV is an arthropod-borne virus, its hosts include a variety of mammals including horses, cattle, swine, and rodents [26]. The viral genome is 11 kb in length and encodes a single glycoprotein (G), a nucleocapsid (N) protein, a polymerase (L) protein, a phosphoprotein (P), and a Matrix (M) protein [26]. VSV G is essential for viral attachment, fusion and budding [27]. The virion binds to Low-Density Lipoprotein Receptors (LDLR) and is then endocytosed into the host cell [28], where pH-dependant fusion of the viral membrane to the endosome

occurs, which releases the ribonucleoprotein, a complex composed of the RNA genome and the VSV P, L, and N proteins, into the cytoplasm [29–31]. The RNA-dependant RNA polymerase (L) forms a complex with its polymerase cofactor (P) and initiates the transcription of viral mRNAs [32,33]. The L protein is also required for the capping, methylation, and polyadenylation of viral transcripts, while the N protein encapsulates the viral RNA and protects it from degradation [34–39]. The M protein is required for proper packaging of virions.

In order to contain infection and protect neighbouring cells, infected normal cells produce antiviral factors in response to infection. Interestingly, VSV M has the capacity to block cellular gene expression at multiple levels and therefore prevents the production of these antiviral factors [40]. Indeed, it has been reported that VSV M inhibits the transcription and nuclear export of cellular mRNA [41–43] as well as the translation of mRNA to functional protein [44,45]. Although VSV M prevents the production of antiviral factors, VSV's tropism towards malignant cells still partially depends on the IFN response [46]. Indeed, VSV's preferential replication in IFN-defective cancer tissue has been well established [44,45]. To further improve VSV's selectivity towards cancer cells, a variant of VSV was created with a deletion of methionine 51 in the M protein (VSVΔ51). This deletion impairs VSV M's ability to block the production of antiviral factors. Consequently, VSVΔ51 is rendered highly sensitive to inactivation in normal cells with an intact antiviral response, but can productively infect cancer cells with a defects in these pathways [47].

1.3 Type I IFN Response

The innate immune response is the first line of defense against invading pathogens. In terms of viral infection, type I IFNs play a major role in mounting the antiviral defense. IFNs are a family of structurally related cytokines with antiviral, anti-tumour, and immunomodulatory functions [48]. Type I IFNs include IFNα and IFNβ, both of which are ubiquitously expressed in most cell types

and up-regulated upon pattern recognition receptor (PRR) stimulation [48]. The regulation of type I IFNs has been studied extensively and it is well established that IFNβ expression is tightly regulated by three sets of transcription factors: IFN regulatory factors 3 and 7 (IRF3/7), activator protein 1 (AP1) (composed of c-jun and ATF2), and nuclear factor kappa–light-chain-enhancer of activated B cells (NFκB) [49] (**Fig 1**). In order to achieve maximal induction of IFNβ, all three transcription factor sets assemble in a complex called the enhanceosome which binds to the IFNβ promoter region and triggers its expression [49]. The following segment will outline the details concerning the initiation and regulation of type I IFN production and response.

1.3.1 PRRs

The host antiviral response is initiated when PRRs are engaged by pathogen-associated molecular patterns (PAMPs). There are several PRRs within the cytoplasm, cell surface, and endosomal membranes that can be activated in response to infection by RNA viruses [50,51]. Of those, Toll-like receptors (TLRs) are a conserved family of transmembrane glycoproteins that reside on the cell surface and endosomal membranes and respond to a variety of PAMPs [50,52]. For example, TLR4 is expressed on the cell surface and responds to viral components such as glycoproteins [53–56], while TLR7 is predominantly located in endosomes where it senses viral RNA and is therefore activated by a variety of viruses including Influenza A virus, human immunodeficiency virus, Sendai virus and VSV [57–60]. Upon stimulation, these TLRs recruit myeloid differentiation primary response gene 88 (MyD88), initiating a downstream signalling cascade [61].

TLRs are not the only receptors responsible for detecting virus particles. In the cytoplasm, retinoic acid-inducible gene-I (RIG-I)-like receptors (RLRs) are the predominant family of PRRs that respond to viral RNA. This family consists of RIG-I, melanoma differentiation-associated antigen 5 (MDA5), and laboratory of genetics and physiology 2 (LGP2) [52]. RIG-I and MDA5 both

contain helicase and caspase activation and recruitment domains (CARD) as well as ATP-binding motifs. Upon infection, the helicase domains recognizes and binds to viral RNA [61]. Binding of viral RNA, combined with binding of ATP, induces a conformational change that exposes the CARD and allows for interaction with the CARD of IFN promoter stimulator 1 (IPS-1), an antiviral mitochondrial transmembrane protein [61]. This ultimately results in the initiation of major signaling intermediates including IRFs, mitogen-activated protein kinases (MAPKs), and NFκB [52], all of which are important for the regulation of both the innate and adaptive immunity.

1.3.2 IRF Signaling

The IRF family of transcription factors include 9 members (IRF1-9) that share extensive homology in their N-terminal DNA-binding domain. IRF3 and IRF7 are amongst the most characterized of the family and are both key regulators of the antiviral response and induce the expression of IFNβ. IRF3 is constitutively expressed at high levels in absence of infection, whereas IRF7 is expressed at much lower levels and is induced by Type I IFNs. Indeed, it is generally thought that IRF3 contributes more to the first wave of IFNβ production [62]. Upon viral infection, both TLR and RLR signalling cascades trigger the phosphorylation of serine/threonine clusters at the C-terminal region of IRF3 [62], which is mediated by two serine/threonine kinases: inhibitor of NFκB kinase ε (IKKε) and TANK-binding kinase-1 (TBK1) [63,64]. Phosphorylation of IRF3 allows for dimer formation (either homodimerization or heterodimerization with IRF7) and interaction with the cofactors cyclic-AMP-responsive-element-binding protein (CREB)-binding protein (CBP) or p300 in the nucleus [65–68]. This complex will then bind to a consensus DNA sequence known as IFN-stimulated response element (ISRE), resulting in the up-regulation of many genes involved in immunity, including IFNβ [69,70].

1.3.3 MAPK Signalling

Upon infection, RIG-I has been demonstrated to activate MAPK kinases 4 and 7 (MKK4 and MKK7), which in turn phosphorylate the MAPK known as c-jun N-terminal kinase (JNK) [71,72]. JNK proceeds to translocate to the nucleus, where it phosphorylates several components of AP-1 including c-jun and ATF2 [73].

The AP-1 transcription factor is a dimeric complex that can be composed of homodimers and heterodimers of Jun, Fos, musculoaponeurotic fibrosarcoma (MAF), and activating transcription factor ATF [74]. Due to its diverse composition, AP-1 is activated by a variety of stimuli including cellular stress, oxidative stress, inflammatory cytokines, ultraviolet radiation, growth factors and infection by pathogens [74]. The AP-1 heterodimer consisting of c-jun and ATF2 is most known for its role in the up-regulation of several pro-inflammatory cytokines including IL-6, IL-8, TNFα, and IFNβ [73].

1.3.4 NFκB Signalling

NFκB is a highly characterized transcription factor, well known for its involvement in many cellular processes including cell proliferation and survival, response to oxidative stress, and innate and adaptive immunity [75]. To date, five NFκB subunits have been identified: p65 (RelA), p105/p50, RelB, c-Rel, and p100/p52 [75]. All five components contain a Rel homology domain (RHD), which is essential for the formation of homo- or heterodimers and binding to DNA elements [75]. A variety of different dimers can be formed in response to different stimuli. These different variations of the pathway have been classified as canonical, non-canonical and atypical. The canonical pathway is most commonly engaged during viral infection, which is mediated by the heterodimer of p65 and p50 and is activated upon stimulation of TLRs, RLRs, and tumour-necrosis factor receptor superfamily (TNFRs) [52]. In quiescent cells, the dimers are sequestered in the

cytoplasm by a family of inhibitory proteins called inhibitors of NFκB (IκB) [75]. IκBs contain ankyrin repeats which bind to the DNA-binding domains of the NFκB transcription factors, rendering them transcriptionally inactive [75]. Upon infection, serine residues on IκB proteins are phosphorylated by a complex of IκB kinases (IKKα, IKKβ, and IKKγ). The phosphorylated IκB molecules are then ubiquitinated by a ubiquitin-conjugating enzyme and a ubiquitin-protein ligase, which flags them for proteasome degradation and frees the NFκB heterodimers [76,77]. The heterodimers then translocate to the nucleus where they bind κB elements and induce a large subset of genes, including pro-inflammatory cytokines such as IL-6, TNFα, and IFNβ [78].

While the canonical NFκB pathway responds to signals elicited by a variety of receptors, the non-canonical pathway is activated by a specific subset of receptors belonging to the TNFR superfamily [79]. These receptors mediate non-canonical NFκB through NFκB-inducing kinase (NIK), which mediates p100 phosphorylation along with IKKα [79]. Upon phosphorylation by NIK, p100 is polyubiquitinated and processed into the p52 subunit [79]. In addition to acting as a precursor for p52, p100 also acts as an inhibitor of RelB and sequesters it in an IκB-like fashion [80]. Upon p100 processing and p52 generation, RelB is released and associates with p52 to form the active transcription factor with a role in regulating lymphoid organogenesis and self-tolerance, secondary lymphoid organ development, B cell development, and bone metabolism [80].

Because of its role as a master regulator of cell cycle, proliferation and inflammation, the NFκB subunits are heavily regulated by many post-translational modifications. The p65 subunit is the most characterized, known to contain more than 11 phosphorylation sites, which impact its stability, nuclear translocation, protein-protein interactions, and transcriptional activity [81–83]. Phosphorylation of p65 can occur both in the cytoplasm and nucleus and is mediated by several kinases including protein kinase A (PKA), mitogen- and stress-activated protein kinase-1 (MSK1),

ribosomal subunit kinase-1 (RSK1), TBK1 and several IKKs [84]. Phosphorylation of p65 can either decrease or increase transcription depending on the phosphorylation sites and the stimuli [84]. In addition to phosphorylation, reversible acetylation has been demonstrated to play a crucial role in the regulation p65 [85–87]. Unlike phosphorylation, acetylation of p65 commonly occurs in the nucleus and is mediated by histone acetyltransferases and histone deacetylases. Reversible acetylation of p65 plays an important role in the regulation of its DNA-binding activity, transcriptional activity and association with IκB molecules [84]. Cysteine modifications have also been shown to play an important role in NFκB regulation [88]. For example, p65 Cys-38 is subject to hydrogen sulfide-linked sulfhydration, which inhibits its transcriptional activity [89]. Cysteines in both p65 and p50 are subject to other modifications including glutathionylation and redox-mediated modifications, which will be discussed further in section 1.5.3. These post-translational modifications are heavily involved in the regulation of NFκB-mediated antiviral response and their effects on NFκB can vary depending on the target genes and stimuli [84].

1.3.5 The JAK-STAT Pathway

Type I IFNs can bind to IFNα/β receptors (IFNARs) in an autocrine or a paracrine fashion, initiating a classical antiviral signalling cascade known as the JAK/STAT pathway. Ligand binding to IFNARs triggers the autophosphorylation of the receptor-associated janus kinase 1 (JAK1) and tyrosine kinase 2 (TYK2) [70,90], which in turn phosphorylate signal transducer and activator of transcription 1 and 2 (STAT1 and STAT2) [70]. Phosphorylated STAT1 and STAT2 then form a heterodimer and associate with IRF9 to form the ISG factor 3 (ISGF3) complex [70]. ISGF3 binds to specific elements known as IFN-stimulated response elements (ISREs), which induces the expression of hundreds of antiviral effectors known as IFN-stimulated genes (ISGs) [70]. ISGs combat viral infection through several mechanisms, including inhibiting virus entry [91–94], virus replication

[95–97], and virus egress [98]. For example, MX dynamin like GTPase 2 (MX2) is an ISG that inhibits human immunodeficiency virus infection by preventing the reverse-transcribed viral genome from entering the nucleus and thereby inhibits its chromosomal integration [99,100]. Another example is IFN-induced transmembrane protein 1 (IFITM1), an ISG that is enriched in endosomes and lysosomes and inhibits a variety of viruses by preventing fusion of the viral membrane with endosomes, a required step for effective entry of many viruses [101,102].

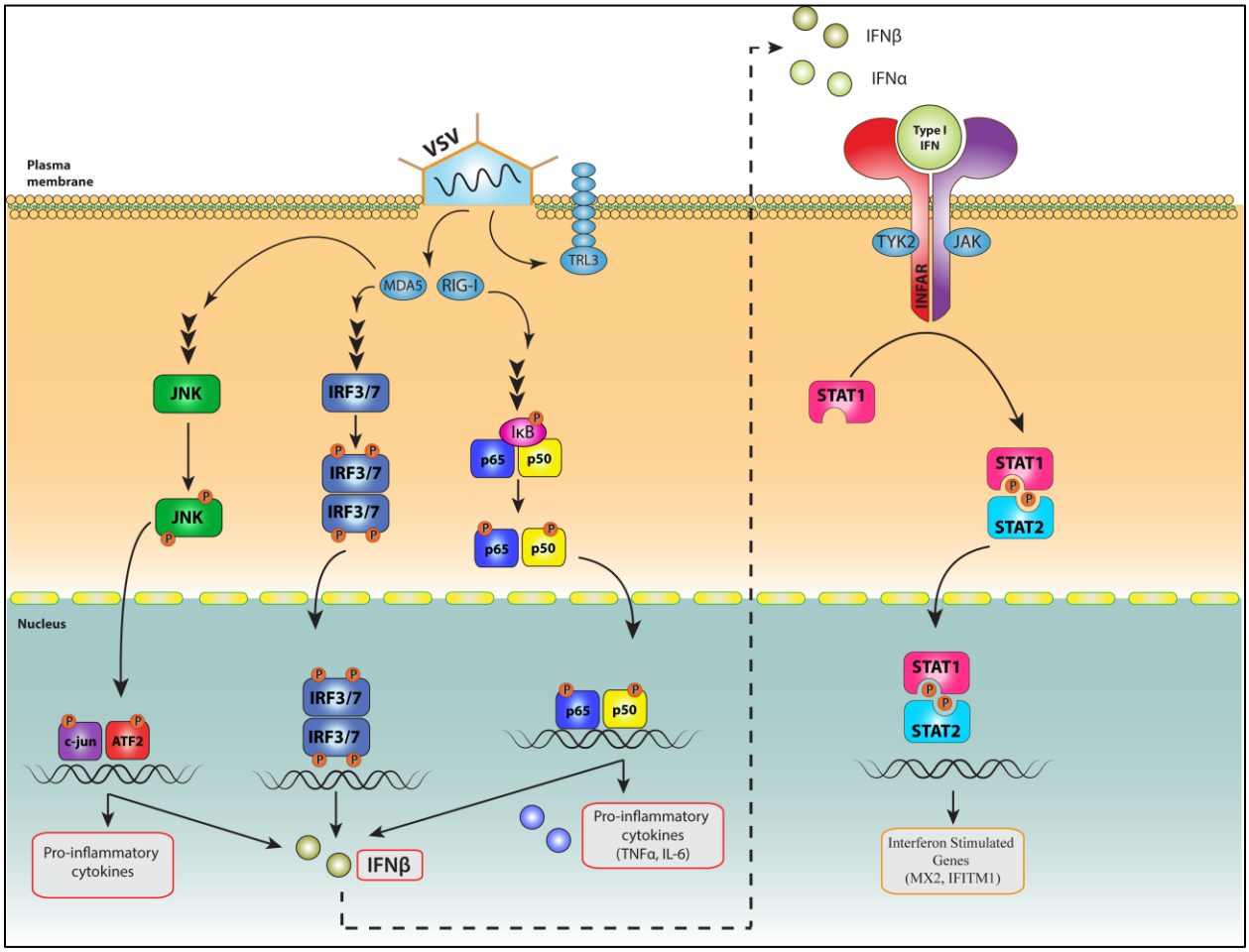

Figure 1. Pathways regulating the production and response to IFNβ.

1.4 Viral Sensitizers

As previously described, OVs are often attenuated to increase their safety profile and selectivity towards cancer cells. However, malignancies are heterogeneous in nature and attenuation can limit viral infection in cancer cells with sufficiently robust antiviral signalling pathways, which is estimated to be the case in approximately one third of cancers. As previously mentioned (section 1.2.1), many strategies have been developed to potentiate the efficacy of OV therapy while maintaining the safety profile. These strategies include bioengineering of OV variants [13,22,103], synergistic combination of OVs with complementary activities [104], and co-treatment with OVs and small molecules that sensitize cancer cells specifically to OV infection and killing (termed viral sensitizers or VSes) [24,25,105,106]. One of the first reported examples of the latter are histone deacetylase (HDAC) inhibitors. Indeed, it has been demonstrated that HDAC inhibitors inhibit IRF3/7 signalling and augment VSV-induced apoptosis in cancer cells [105]. More recently, microtubule-destabilizing agents have also been used in combination with OVs. The mechanism of these compounds is two-fold: the microtubule destabilizers disrupt type I IFN translation and also increase viral bystander killing by promoting cell death following stimulation by virus-induced cytokines [106].

1.4.1 VSe1

One promising synthetic small molecule, Viral Sensitizer 1 or VSe1 (3,4-dichloro-5-phenyl-2,5-dihydrofuran-2-one), has been shown to enhance VSV replication and spread up to 1,000-fold in cancer cell lines [107]. This small molecule was identified alongside microtubule destabilizers following screening of a large chemical library to identify compounds capable of enhancing the oncolytic activity of VSVΔ51. VSe1 was found to be the most efficacious viral sensitizer in *vitro* from those initial screens performed in resistant mouse breast cancer cells. VSe1 was also tested in combination with VSVΔ51 in non-malignant cells and has been shown to maintain the selectivity of VSVΔ51 for cancer cells [107]. I*n vivo,* it was demonstrated to significantly delay tumour

progression and prolong survival [107]. While the molecular target responsible for the viral sensitizing properties of VSe1 is still unknown, early experiments showed that VSe1 represses 96% of VSV-induced antiviral transcripts, many of which are ISGs. Furthermore, VSe1 was shown to dampen the response to exogenous IFNα in a human glioma cell line [107]. Altogether these data suggest that VSe1 either directly or indirectly targets key components of type I IFN signalling.

1.4.2 VSe1 Structural Analogues

Although VSe1 was a first and novel hit specifically identified for combination therapies with OVs, there are several drawbacks that hinder its translational potential. Namely, the electrophilic nature of VSe1 makes it unstable in aqueous media at physiological pH, making the compound difficult to use therapeutically. Furthermore, VSe1 has poor solubility and is not well tolerated in animals. As a result, over 100 structural analogues of VSe1 have been synthesized in a structure-activity relationship approach to optimize physiochemical properties while maintaining the efficacy and selectivity of VSe1. Over 50 of these analogues were tested *in vitro* and shown to be effective and cancer-selective enhancers of VSVΔ51 infection [108]. The analogues were categorized based on their heterocycle scaffold (furans and pyrroles) (**Fig 2**). The results showed that the pyrrole analogues had vastly improved physiochemical and toxicological properties relative to the furan compounds, but had equal or superior capacity to enhance cancer-specific viral growth compared to VSe1 in *in vitro* and *ex vivo* assays [108]. VSe1-28 (*H*-Pyrrol-2-one, 3,4-dichloro-1,5-dihydro-5-hydroxy-1-[2-(4-morpholinyl)ethyl]) was selected as a lead candidate for further assessment in combination with OV treatment *in vivo*. Similarly to VSe1, VSe1-28 significantly delayed tumour progression and prolonged survival in tumour-bearing mice in combination with VSVΔ51 [108]. Furthermore, VSe1-28 was tolerated in mice at doses up to 100 mg/kg, which is a great improvement compared to VSe1 which is toxic at doses exceeding 20 mg/kg.

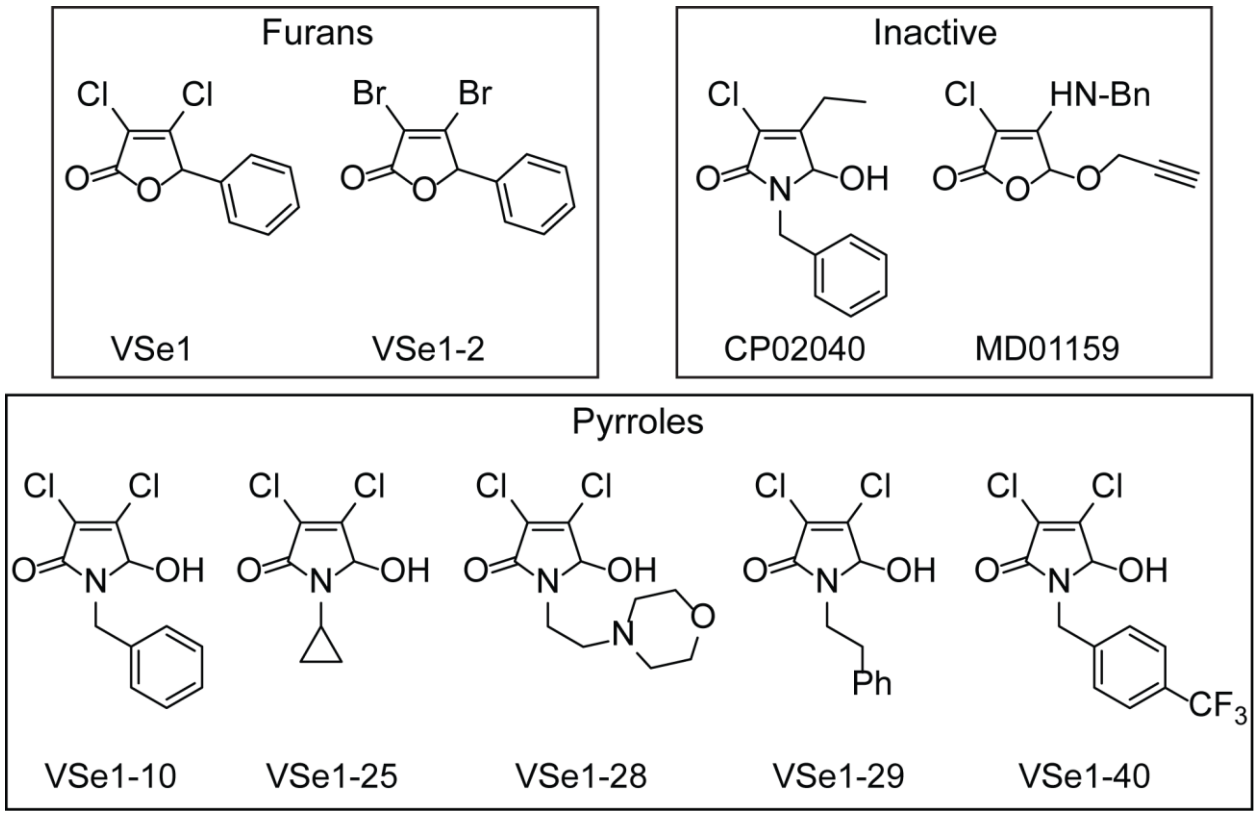

Figure 2. VSe1 and its structural analogues.

1.5 Glutathione Homeostasis

In addition to providing more drug-like candidates, the structural analogues of VSe1 were used to gain insight into the molecular target(s) of these compounds. Inhibitor affinity capture experiments were carried out revealing that VSe1 analogs interact with glutathione (GSH)-s-transferase-π (GSTP1). Furthermore, VSe1 and its analogues were demonstrated to react with supra-physiological concentrations of free glutathione (GSH) [108] and inhibit the enzymatic activity of GSTP1 (Krishnan/El Sayes et al. Manuscript in preparation).

1.5.1 Role of GSH and GSTs

GSH (L-γ-glutamyl-L-cysteinylglycine) is a tripeptide best known for its role in detoxification of reactive electrophiles and xenobiotics [109]. The tripeptide is composed of cysteine,

glutamic acid, and glycine, and its active component is the thiol group of the cysteine portion. GSH regulates redox homeostasis by acting as an antioxidant, either through direct interactions with reactive oxygen species (ROS) and electrophiles, or by acting as a cofactor for detoxification enzymes [109]. Free GSH is generally present in its reduced form, however it becomes oxidized during periods of oxidative stress. The ratio of reduced and oxidized GSH is often used as a measurement of oxidative stress within the cell [109]. Because of its role in cell detoxification, high levels of cellular GSH is often the cause of drug resistance. Indeed, several reports demonstrate that resistant cancer cells can be sensitized to anti-tumour agents and radiation by inhibiting GSH biosynthesis, which can be done for example by treatment with buthionine sulfoximine (BSO) [110–112].

Conjugation of GSH to electrophiles is often catalyzed by glutathione-S-transferases (GSTs). There are 7 different classes of GSTs: alpha (A), mu (M), pi (P), sigma (S), theta (T), omega (O), and zeta (Z) [113]. Most classes of GSTs include several subunits, with some containing up to 5 distinct subunits [113]. While GSTs are most known for their role in detoxification, they are also involved in the regulation of several pathways, either by interacting with proteins directly or by regulating a post-translational modification known as S-glutathionylation [114,115]. Indeed, GSTs have been shown to participate in regulating MAPK pathways that control cell proliferation, cell death, and innate immunity [113]. One such example is the inhibition of JNK activity by GSTP1 in a MKK4-independent manner [116].

1.5.2 Regulation of Protein Activity by S-Glutathionylation

S-glutathionylation is a redox-dependent post-translational modification that involves the conjugation of GSH to redox-sensitive cysteine residues on proteins by disulfide bond [117]. This bond is reversible, which is a key element of the regulatory function of protein glutathionylation. The process of deglutathionylation is carried out by the enzyme glutaredoxin (GRX), although the

enzyme is also capable of catalyzing protein glutathionylation under specific conditions [117]. During the past decade, more research has focused on establishing the role of protein glutathionylation in regulating many cellular processes including pathways involved in gene expression [118–120], cell death and survival [121,122], and energy metabolism and glycolysis [123–126].

1.5.3 Glutathionylation and Viral Defense

Many pathways involved in innate immunity can be regulated by protein glutathionylation. For example, one group has demonstrated that IRF3 is normally glutathionylated in resting cells. Upon infection, GRX-mediated deglutathionylation of IRF3 was shown to be necessary for its interaction with the cofactor CBP, and subsequent expression of IFNβ [120]. Glutathionylation has also been reported to regulate various components of the NFκB pathway. The kinase activity of IKKβ is inhibited by glutathionylation of one of its cysteine residues (Cys-179), which results in dampened TNFα-induced NFκB activation [127]. IκBα is another component that can be glutathionylated, which inhibits its phosphorylation and subsequent ubiquitination. This prevents the degradation of IκBα and keeps the NFκB complex sequestered in the cytoplasm [128]. The NFκB transcriptional subunits are also susceptible to glutathionylation. For example, the p50 subunit contains a redox-sensitive cysteine (Cys-62) in its DNA-binding domain, which upon glutathionylation inhibits its DNA-binding activity [129]. Furthermore, several reports have demonstrated that glutathionylation of p65 at Cys-38 inhibits both its nuclear translocation and its DNA-binding activity, and that inducers of protein glutathionylation (i.e. GSH supplementation, GRX inhibitors, N-acetyl-L-cysteine treatment) inhibit NFκB activity [130–132].

1.6 Rationale and Hypothesis

The heterogeneity of the tumour microenvironment constitutes a major hurdle to OV-therapy. The use of VSes as potentiators of OV-therapy is one of the several strategies currently being developed for enhancing the efficacy of the treatment while maintaining a favourable therapeutic index. Although VSe1 and its analogues show therapeutic promise pre-clinically, we still lack a comprehensive understanding of the mechanism of action responsible for the viral sensitizing properties. Uncovering the precise mechanism of action is critical for the continued development of combination therapies that synergize with OV-therapy as well as the development of new generations of optimal VSes. Furthermore, this knowledge is imperative for eventual clinical testing.

Our previous data suggest that VSe1 and its structural analogues affect the type I IFN antiviral response and have the potential to affect cellular redox homeostasis. Based on these results and given the importance of both pathways for the cellular antiviral defense, **we hypothesize that VSe1 and its structural analogues potentiate VSVΔ51 activity by inhibiting the type I IFN response via redox-mediated dysregulation**. Our main objective was to uncover the mechanism of action of VSe1 and its analogues. To do this, we first set out to characterize the effect of VSe1 and its analogues on the innate antiviral response to identify target proteins. Upon identification of potential targets, we investigated the relationship between regulation of redox homeostasis by the VSes and their inhibition of the innate antiviral response.

2. Materials and Methods

2.1 Cell Lines

786-0 (human renal carcinoma), Vero (monkey kidney), and 293T (human embryonic kidney) were obtained from the American Type Culture Collection (Manassas,VA) and maintained in Dulbecco's Modified Eagle's medium (Corning, Manassas, VA) supplemented with 10% fetal bovine serum (Sigma-Aldrich, St Louis, MO) and buffered with 30 mM HEPES (Thermo Fisher Scientific, Waltham, MA). All cell lines were maintained at 37 °C with 5% CO_2 in a humidified incubator.

2.2 Viruses

A recombinant variant of the Indiana serotype of VSV harbouring a deletion of the methionine 51 in the M protein (VSVΔ51) was used throughout this study. VSVΔ51 expressing green fluorescent protein (VSVΔ51-GFP) is a variant that has been previously described by Stojdl *et al* [47]. Viruses were propagated on Vero cells and purified by 0.22μM filtration and ultracentrifugation on an Optiprep gradient. Virus quantification was performed by plaque assay as previously described [133].

2.3 Drugs and Cytokines

The synthesis of VSe1 and its analogs (VSe1-2, VSe1-6, VSe1-10, VSe1-25, VSe1-27, VSe1-28, VSe1-29, VSe1-40, MD02172, CP02040) was done in the laboratory of Dr. Christopher Boddy as described by Dornan *et al* [108]. Buthionine sulfoximine (BSO), Bay 11-7085, N-aceylcysteine (NAC), and cinnamaldehyde were obtained from Sigma-Aldrich (St Louis, MO). H_2O_2 was obtained from Fisher Scientific (Fair Lawn, NJ). IFNβ was obtained from PBL Interferon Source (Piscataway, NJ) and TNFα from R&D systems (Minneapolis, MN).

2.4 Plaque Assay

Virus quantification was done by plaque assay and is thoroughly described in Diallo *et al* [133]. Briefly, samples were serially diluted and incubated on Vero cells. The supernatants were then removed and a 1:1 mixture of 1% agarose in 2x high glucose DMEM (12800017, Life Technologies, Carlsbad, CA) supplemented with 20% fetal bovine serum (Sigma-Aldrich, St. Louis, MO), 30 mM HEPES (Sigma-Aldrich, St. Louis, MO) is immediately added. The inoculated cells are then incubated at 37°C in a 5% CO_2 humidified incubator for 24 hours, after which the cells are fixed in 3:1 methanol: acetic acid and stained with a Coomassie Brilliant Blue R-250 (Sigma-Aldrich, St. Louis, MO) solution containing 0.5 g Coomassie blue, 20% methanol and 10% acetic acid. The plaques are counted and the virus titers are calculated based on the dilution and reported as plaque forming units (pfu) per millilitre.

2.5 Luciferase-Based Viral Titration Assay

This assay has previously been described in detail [134]. Briefly, supernatants from samples infected with VSVΔ51-FLuc were added Vero cells seeded in white-bottom 96 well plates (Corning, Kennebunk, ME, USA). At the same time, known amounts of virus (starting at $1x10^8$ plaque forming units (pfu) and decreasing by 1 log unit to 10 pfu) were added to adjacent columns on the plate to generate a standard curve. Plates were centrifuged at 430xg for 5 minutes and then incubated for 5 hours at 37°C. Luciferase expression was then measured and bioluminescence was expressed in mean relative light units (mRLU; SynergyMx Microplate Reader, BioTek). To generate the standard curve, mRLU was plotted against known input pfu. Four-parameter non-linear regression analysis generated a Hill plot from which unknown input pfu (estimate of viral titer) was interpolated. Data transformation was conducted in R. These estimated titers are termed “viral expression units” (VEU).

2.6 Western Blot Analysis

Cells were lysed for 10 minutes on ice in protein extraction buffer (50mM HEPES, 150mM NaCl, 10mM EDTA, 10mM $Na_4P_2O_7$, 1% NP-40 pH 7.4) supplemented with 1M NaF, 200mM Na_3VO_4 and protease inhibitor cocktail (Roche, Mississauga, Ontario, Canada) [135]. Whole cell lysates were centrifuged at 16,000 g for 10 minutes at 4°C.

For separation of nuclear and cytoplasmic fractions NE-PER^{TM} nuclear and cytoplasmic extraction reagents (Pierce Biotechnology, Rockford, IL) were used as per the manufacturer's protocol. Following protein determination by Bradford assay (Protein Assay Solution, BioRad, Mississauga, Ontario) 20-50 µg of protein extracts were prepared in NuPAGE LDS sample buffer (Invitrogen, Burlington, Ontario) supplemented with dithiothreitol and the lysates were then electrophoresed on a 4-12% precast gradient gel (Invitrogen, Burlington, Ontario) using the XCell *SureLock*® Mini-cell (Invitrogen, Burlington, Ontario) and transferred onto a nitrocellulose membrane (GE Healthcare, Baie d'Urfe, Quebec). The membranes were blocked with 5% BSA or 5% non-fat dry milk in 0.1% TBS-Tween-20 for at least 1h at RT and probed with rabbit or mouse antibodies against NFκB p65, phospho-NFκB p65, NFκB p105/p50, IRF-3, phospho-IRF-3, c-jun, phospho-c-jun, ATF2, phospho-ATF2, IκBα, β-Actin (all from Cell Signalling Technology, Danvers, MA), α-Tubulin (Santa Cruz Biotechnology, Dallas, Texas) or glutathionylated proteins (ab19534, Abcam, Toronto, ON) overnight at 4°C. In the case of probing for glutathionylated proteins, cells were lysed under non-reducing conditions (no dithiothreitol or β-mercaptoethanol). The membranes were then washed and probed with horseradish-peroxidase conjugated anti-rabbit (Jackson Immunoresearch Labs, West Grove, PA) or anti-mouse (Cell Signalling Technology, Danvers, MA) secondary antibodies for 1h at RT. Blots were washed and bands were visualized

using Clarity™ Western ECL blotting substrates (Bio-Rad, Mississauga, Ontario) on HyBlot CL autoradiography films (Denville Scientific, Holliston, MA).

Manufacturer	Antibody	Catalogue #	Dilution
Cell Signaling	NFκB p65	8242	1:1000
Cell Signaling	Phospho NFκB p65	3033	1:1000
Cell Signaling	NFκB p105/p50	3035	1:1000
Cell Signaling	IRF3	11904	1:1000
Cell Signaling	Phospho IRF3	4947	1:1000
Cell Signaling	c-jun	9165	1:1000
Cell Signaling	Phospho c-jun	9261	1:1000
Cell Signaling	ATF2	9226	1:1000
Cell Signaling	Phospho ATF2	9221	1:1000
Cell Signaling	IκBα	4814	1:1000
Cell Signaling	β-Actin	4970	1:1000
Santa Cruz	α-Tubulin	8035	1:500
Abcam	Glutathione	19534	1:500

2.7 Immunoprecipitation

250 µl of cell lysates were pre-cleared with protein G Dynabeads (Invitrogen, Burlington, Ontario) for 30 min at RT. Beads were replaced with fresh protein G Dynabeads and rabbit-anti NFκB p65 antibody (Cell Signalling Technology) was added to the lysates at 1:250 for one hour at RT. The beads were pelleted and washed three times with 1x lysis buffer prior to eluting with 100mM glycine pH 2.8 and prepared in NuPAGE LDS sample buffer (Invitrogen, Burlington, Ontario) supplemented with dithiothreitol for western blot analysis. In the case of probing for glutathionylated proteins, cells were lysed under non-reducing conditions (no dithiothreitol or β-mercaptoethanol).

2.8 Quantitative Real-Time PCR

RNA extraction was performed using RNeasy® Mini Kit (Qiagen, Valencia, CA) according to the manufacturer's protocol. Then, 1 µg of purified RNA was reverse transcribed using RevertAid H Minus First Strand cDNA Synthesis Kit (Thermo Fisher Scientific, Waltham, MA). Real-time PCR reactions were performed with QuantiTect® SYBR® Green PCR Kit (Qiagen, Valencia, CA) on a 7500 Fast Real-Time PCR system (Applied Biosystems, Foster City, CA) with 20ng of cDNA. Relative mRNA expression was normalized to GAPDH and fold induction was calculated relative to the untreated/uninfected controls using the Pfaffl method [136].

Model	Gene	Forward Primer (5' → 3')	Reverse Primer (5' → 3')
Human	*MX2*	GAACGTGCAGCGAGCTTGTC	AAGGCTTGTGGGCCTTAGAC
Human	*IFITM1*	CCGTGAAGTCTAGGGACAGG	GGTAGACTGTCACAGAGCCG
Human	*IFNβ*	CATTACCTGAAGGCCAAGGA	CAGCATCTGCTGGTTGAAGA
Human	*TNFα*	GCTGCACTTTGGAGTGATCG	GAGGGTTTGCTACAACATGGG
Human	*IL-6*	ACCCCCAATAAATATAGGACTGGA	GAAGGCGCTTGTGGAGAAGG
Human	*HMOX1*	ACTGCGTTCCTGCTCAACAT	GGGGCAGAATCTTGCACTTT
Human	*OSGIN*	GTTCCCCTGACCCTCCTAGT	GGCCGTTACCCACAATGATG

2.9 ELISA

786-0 cells were seeded at a density of 250,000 cells/well in 12-well plates and incubated overnight at 37°C in a 5% CO_2 humidified incubator. Cells were then pretreated with VSes for 2 hours prior to infection with VSVΔ51-GFP at an MOI of 1. Supernatants were collected 8, 16 and 24 hours post-infection. Verikine human IFNβ ELISA kit (PBL Interferon Source) and Quantikine human TNFα ELISA kit (R&D Systems) were used following the manufacturer's protocol. Levels of secreted IFNβ and TNFα (pg/mL) were interpolated from experimental standard curves.

2.10 Microarray

786-0 cells seeded at a density of 1 x 10^6 cells in 6-well plates (Costar). 24 hours later, cells were treated with VSe1 (55 μM), VSe1-2 (55 μM), VSe1-6 (50 μM), VSe1-40 (55 μM), VSe1-28 (95 μM), VSe1-29 (95 μM), VSe1-25 (95 μM), MD02172 (150 μM), CP02040 (150 μM), media or vehicle (DMSO). RNA was collected 24 hours post-infection as explained above. Biological triplicates were subsequently pooled and RNA quality was measured using Agilent 2100 Bioanalyzer (Agilent Technologies) before hybridization. Hybridization to Affymetrix Human PrimeView Array was performed by The Centre for Applied Genomics at The Hospital for Sick Children, Toronto, Canada. Microarray data was processed using Transcriptome Analysis Console (TAC) 3.0 under default parameters of Gene Level Differential Expression Analysis. Fold change in gene expression was calculated for each gene in relation to uninfected, untreated control. Gene ontology (GO)-term enrichments were evaluated using GOrilla [137].

2.11 GSH and GSSG Determinations by HPLC

Levels of GSH, GSSG and their ratio were determined with an Agilent HPLC system [138]. Cells were grown in 60mm tissue culture plates with the indicated treatments. Cells were then washed twice with ice cold PBS and lysed on ice for 20 minutes in 125mM sucrose, 1.5mM EDTA, 5mM Tris, 0.1% TFA and 0.5% MPA in mobile phase (10% HPLC grade methanol, 0.09% TFA – 0.2 micron filtered). Lysates were clarified by centrifugation for 20 min at 14,000 g at 4°C. Each sample was run in duplicate on a Pursuit5 C18 column (150 × 4.6 mm, 5 μm; Agilent Technologies, Santa Clara, CA) with a 1 mL/min flow rate and detected at 215nm. Standards were prepared at the indicated concentrations in the same buffer and used to interpolate absolute quantities of GSH and GSSG in the samples.

2.12 IFNβ Protection Assay

786-0 cells were plated at a density of 250,000 cells/well in 12-well plates and incubated overnight at 37°C in a 5% CO_2 humidified incubator. Cells were cotreated with VSe1 (60 μM) or VSe1-28 (90 μM) and IFNβ (200 U/mL), then challenged with VSVΔ51 at an MOI of 0.01. Supernatants were collected 40 hours post infection and viral outputs were quantified by plaque assay as above.

2.13 Statistical Analysis

The results shown are presented as means ± standard error. For all experiments, statistical significance was considered to mean a P value less than or equal to 0.05. Graphs and statistics were computed using Graphpad Prism 6 and Microsoft Excel.

3. Results

3.1. VSe1 Structural Analogues Supress Response to IFNβ

Previously published data demonstrated that VSe1 blocks the response to type I IFNs [107], however, whether its structural analogues have similar effects has not yet been assessed. To investigate this possibility, 786-0 human renal carcinoma cells were co-treated with VSe1 analogues and IFNβ prior to VSVΔ51 challenge. In the absence of exogenous IFNβ, all the analogues of VSe1 tested enhanced virus production up to 100-fold (**Fig 3**). Treatment with IFNβ prior to infection severely hindered infection, however VSe1 and its structural analogues still enhanced virus production, albeit to varying extents. To further characterize the effects of VSe1 and its structural analogues on the antiviral response, a microarray was performed on samples from 786-0 cells pretreated with active and inactive VSe1 analogues prior to VSVΔ51 infection. As expected, a large subset of genes contained within the GO term "cellular defense response" were upregulated by VSVΔ51. Furthermore, the expression of those genes was inhibited by the active, but not the inactive compounds tested (**Fig 4**). To further characterize the kinetics of ISG inhibition by VSes, we chose two ISGs (MX2 and IFITM1) that were previously studied with VSe1 [107]. Gene expression was assessed by quantitative RT-PCR on samples treated with either VSe1 or VSe1-28 then infected with VSVΔ51 for 8, 16 and 24 hours. As expected, the expression of MX2 and IFITM1 was highly upregulated by infection, however both VSe1 and VSe1-28 dampened the expression of the both ISGs (**Fig 5a & b**).

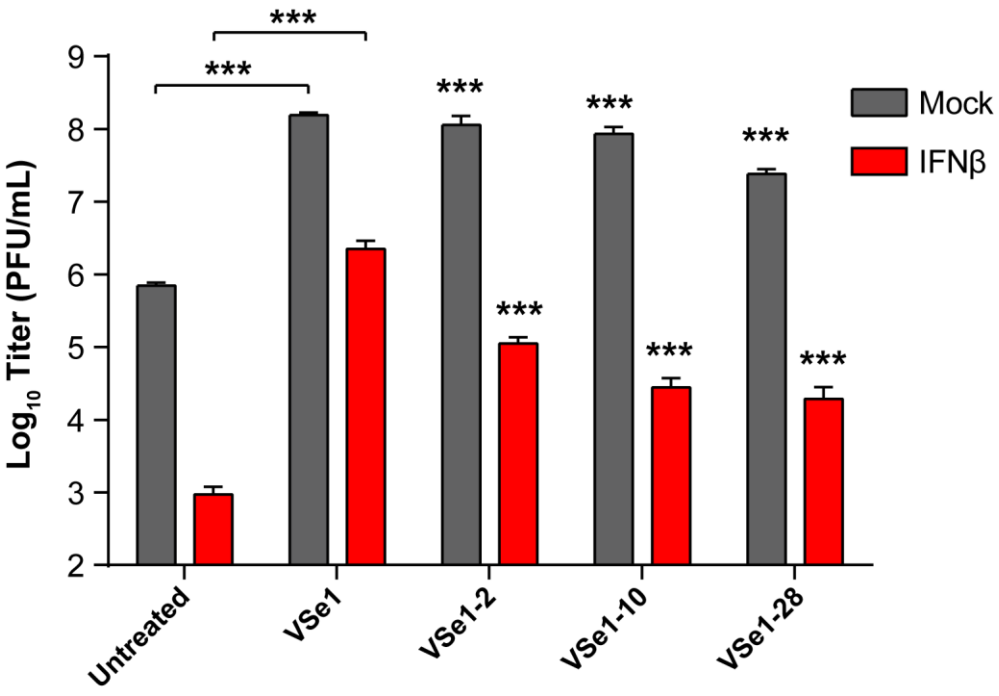
***
***
***
***
***
***
***
***
***
***
Mock
IFNβ
Log10 Titer (PFU/mL)
9
8
7
6
5
4
3
2
Untreated
VSe1
VSe1-2
VSe1-10
VSe1-28

Figure 3. VSe1 suppresses the response to IFNβ. Virus titers from supernatants of cells co-treated with VSe1 analogues and IFNβ then challenged with VSVΔ51 (MOI 0.01) for 40 hours. Concentrations: VSe1 (60 μM), VSe1-2 (50 μM), VSe1-10 (50 μM), VSe1-28 (90 μM). Conditions from each group (i.e. Mock and IFNβ) were compared to their relative untreated control. ***P < 0.001 (Two-way ANOVA with Bonferroni multiple comparison).

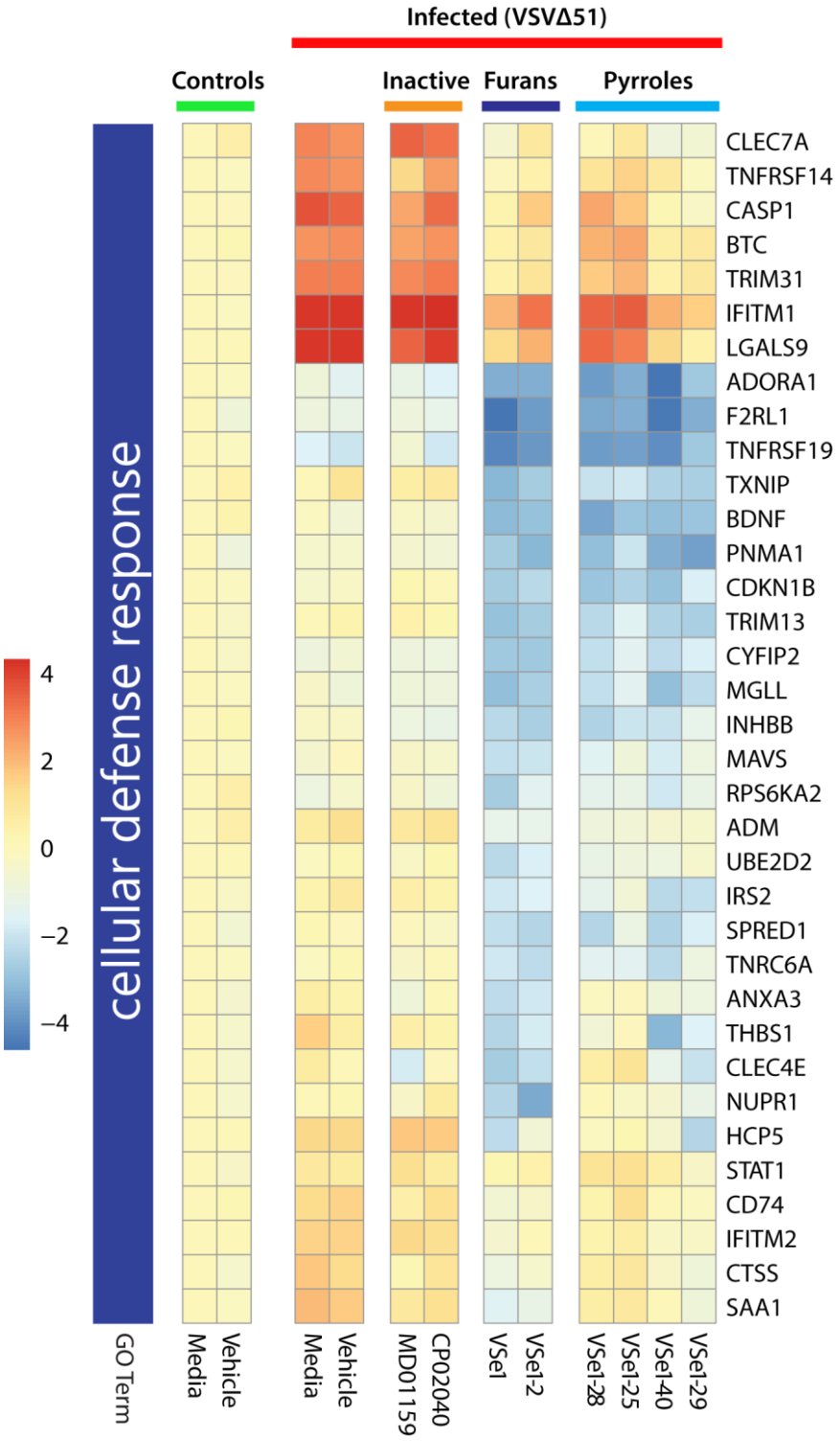
Infected (VSVΔ51)
Controls
Inactive
Furans
Pyrroles
cellular defense response
4
2
0
−2
−4
CLEC7A
TNFRSF14
CASP1
BTC
TRIM31
IFITM1
LGALS9
ADORA1
F2RL1
TNFRSF19
TXNIP
BDNF
PNMA1
CDKN1B
TRIM13
CYFIP2
MGLL
INHBB
MAVS
RPS6KA2
ADM
UBE2D2
IRS2
SPRED1
TNRC6A
ANXA3
THBS1
CLEC4E
NUPR1
HCP5
STAT1
CD74
IFITM2
CTSS
SAA1
GO Term
Media
Vehicle
Media
Vehicle
MD01159
CP02040
VSe1
VSe1-2
VSe1-28
VSe1-25
VSe1-40
VSe1-29

Figure 4. VSe1 analogues supress the expression of antiviral genes. Microarray analysis using RNA from 786-0 cells pretreated with media, vehicle (DMSO), or viral sensitizer, then infected with VSVΔ51 (MOI 0.01) for 24 hours. Triplicates were pooled and hybridized on Affymetrix Human PrimeView Array. Shown are heat maps of genes contained within the GO term "cellular defense response".

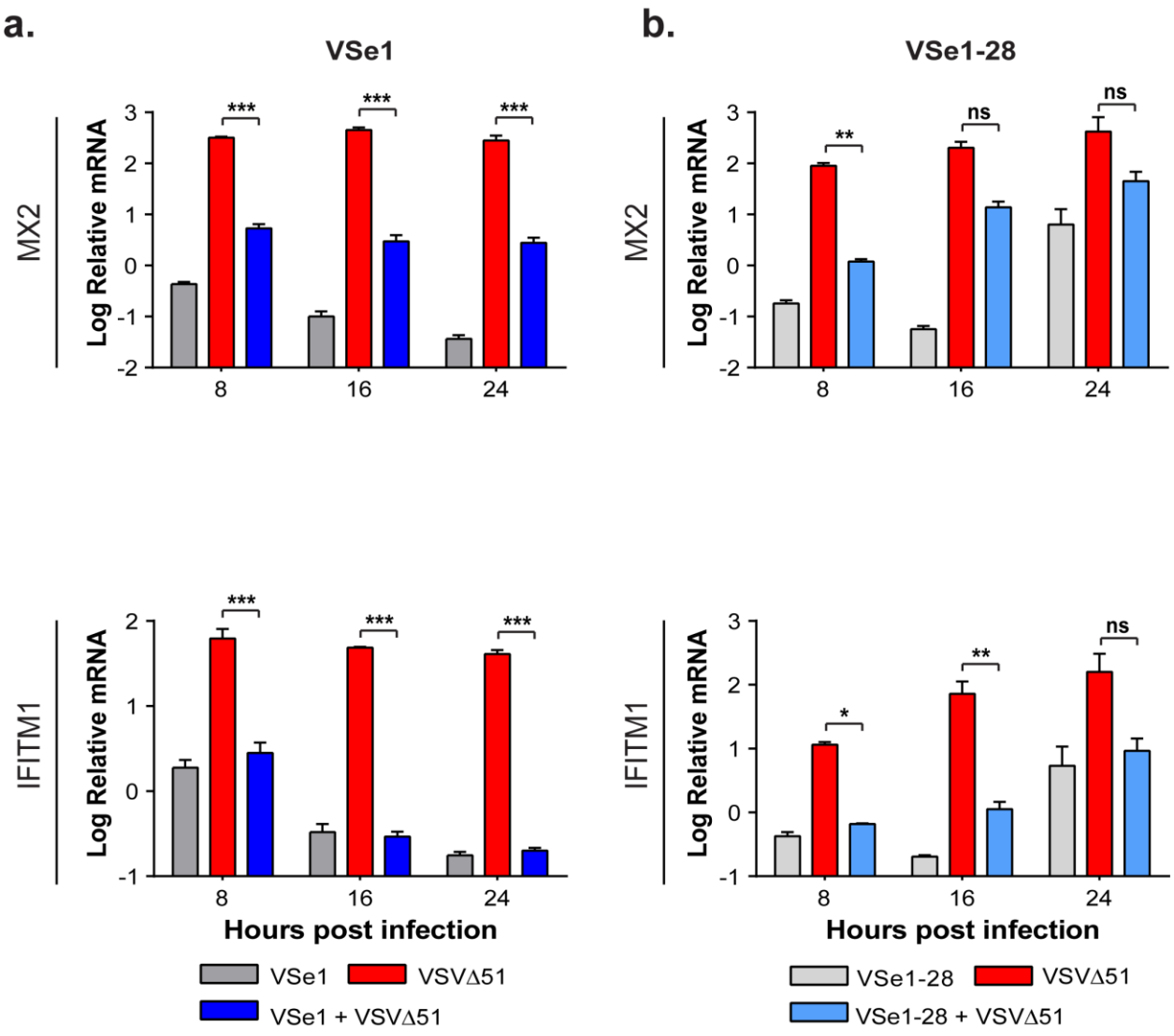
a.
VSe1
MX2
Log Relative mRNA
***
***
***
3
2
1
0
-1
-2
8
16
24
IFITM1
Log Relative mRNA
***
***
***
2
1
0
-1
8
16
24
Hours post infection
VSe1
VSVΔ51
VSe1 + VSVΔ51
b.
VSe1-28
MX2
Log Relative mRNA
**
ns
ns
3
2
1
0
-1
-2
8
16
24
IFITM1
Log Relative mRNA
*
**
ns
3
2
1
0
-1
8
16
24
Hours post infection
VSe1-28
VSVΔ51
VSe1-28 + VSVΔ51

Figure 5. VSe1 and VSe1-28 inhibit antiviral ISGs. Quantitative RT-PCR analysis using RNA from 786-0 cells treated with **(a)** VSe1 (60 μM) or **(b)** VSe1-28 (90 μM) then infected with VSVΔ51 (MOI 1). RNA was extracted 8, 16 and 24 hours post-infection and the expression of MX2 and IFITM1 were determined. ns: $P > 0.05$, *$P < 0.05$, **$P < 0.01$, ***$P < 0.001$ (Two-way ANOVA with Dunnett's multiple comparison).

3.2 Furan Viral Sensitizers Inhibit IFNβ-Mediated STAT1 Activation

As an attempt to identify the mechanism by which the analogues dampen the anti-viral response, and given the known involvement of the JAK-STAT pathway in regulating the expression of ISGs induced by type I IFNs, we examined the phosphorylation status and activation of STAT1. To do so, 786-0 cells were treated with VSe1 or its analogues prior to IFNβ stimulation to specifically activate the JAK-STAT pathway. As expected, IFNβ treatment induced the phosphorylation of STAT1. Interestingly, this phosphorylation was partially inhibited by VSe1 as well as the other furan analogue VSe1-2, however the pyrrole analogues (VSe1-28, 29 & 20) had no impact on the phosphorylation status of STAT1 (**Fig 6**). Taken together, our data suggests that the VSe-mediated decrease in ISG expression and the antiviral effects of IFNβ cannot be consistently explained by blockage of the JAK-STAT pathway.

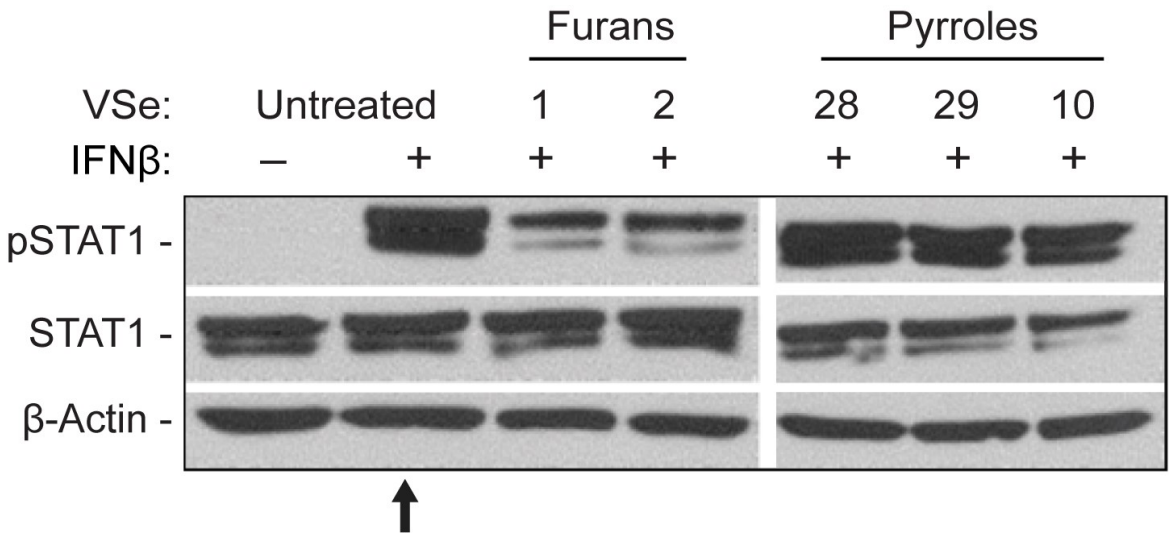
Furans
Pyrroles
VSe:
Untreated
1
2
28
29
10
IFNβ:
–
+
+
+
+
+
+
pSTAT1 -
STAT1 -
β-Actin -

Figure 6. Furan VSes inhibit IFNβ-mediated STAT1 phosphorylation. STAT1 phosphorylation status was analyzed by western blot using whole cell lysates from 786-0 cells treated with VSe1 and analogues for two hours prior to treatment with IFNβ. Lysates were collected 30 minutes later. Arrow indicates IFNβ-treated control. Pyrroles and Furans were on the same blot, which contained other samples, and can be directly compared to the untreated controls.

3.3 VSe1 Analogues Inhibit Expression of IFNβ.

We next investigated the effect of VSe1 analogues on the production of IFNβ. To do so, 786-0 cells were pre-treated with either VSe1 or VSe1-28 then infected with VSVΔ51 for 8, 16 and 24 hours. RT-PCR analysis revealed that VSe1 and VSe1-28 inhibited virus-induced expression of IFNβ for up to 24 hours or 16 hours post-infection respectively (**Fig 7a & b**). Additionally, an ELISA performed on culture supernatants confirmed the impaired production of IFNβ in the presence of VSe-1 and 1-28 as well as other pyrrole analogues (VSe1-10) (**Fig 7c**).

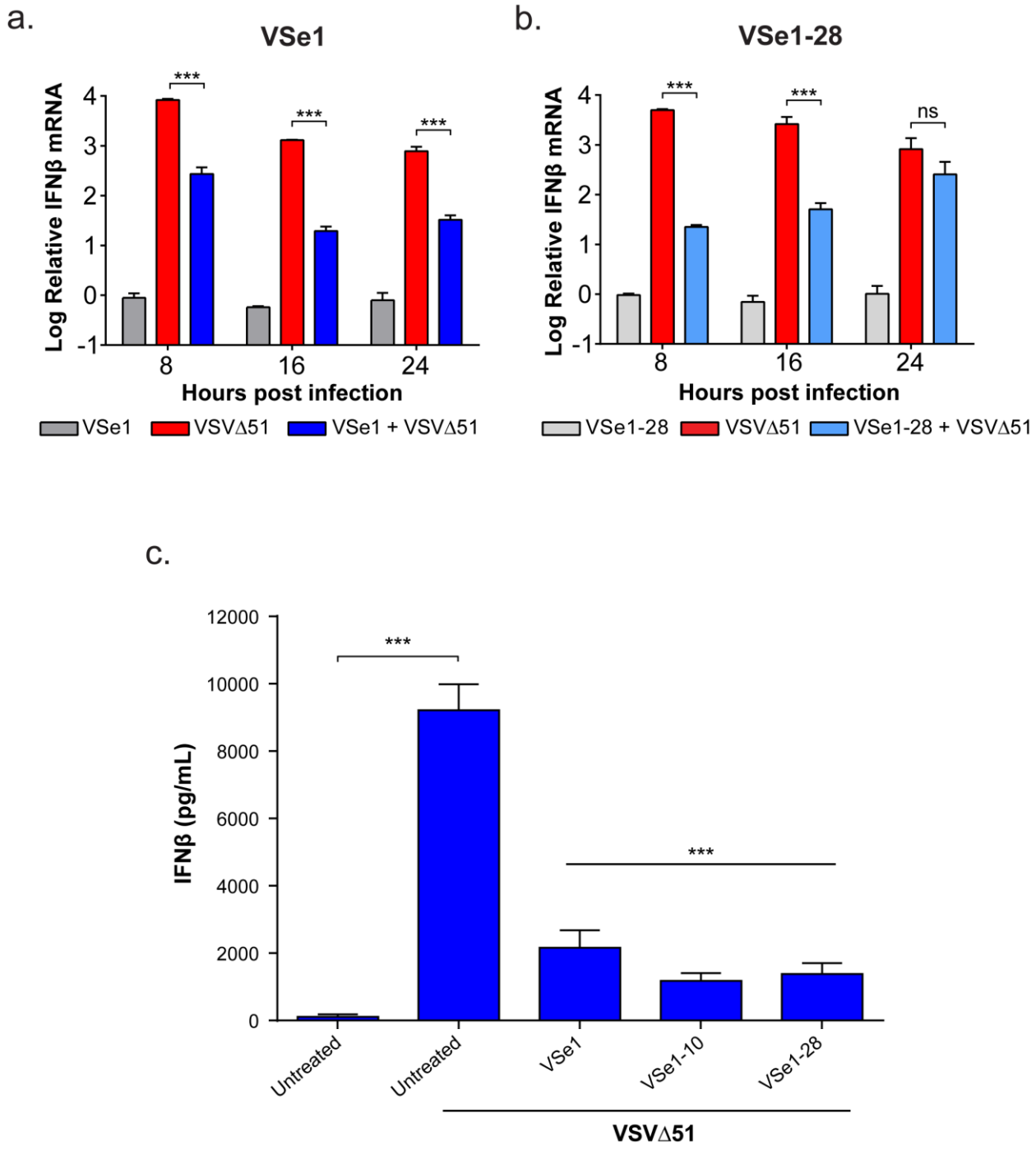
a.
VSe1
Log Relative IFNβ mRNA
4
3
2
1
0
-1
***
***
***
8
16
24
Hours post infection
VSe1
VSVΔ51
VSe1 + VSVΔ51
b.
VSe1-28
Log Relative IFNβ mRNA
4
3
2
1
0
-1
***
***
ns
8
16
24
Hours post infection
VSe1-28
VSVΔ51
VSe1-28 + VSVΔ51
c.
IFNβ (pg/mL)
12000
10000
8000
6000
4000
2000
0
***
***
Untreated
Untreated
VSe1
VSe1-10
VSe1-28
VSVΔ51

Figure 7. VSe1 analogues inhibit the expression of IFNβ. Quantitative RT-PCR analysis using RNA from 786-0 cells treated with **(a)** VSe1 (60 μM) or **(b)** VSe1-28 (90 μM) then infected with VSVΔ51 (MOI 1). RNA was extracted 8, 16 and 24 hours post-infection and the expression of IFNβ was determined. ns: $P > 0.05$, *$P < 0.05$, **$P < 0.01$, ***$P < 0.001$ (Two-way ANOVA with Dunnett's multiple comparison). **(c)** IFNβ production was measured by ELISA using supernatants from 786-0 cells treated with VSe1 (60 μM), VSe1-10 (50 μM), or VSe1-28 (90 μM) then infected with VSVΔ51 (MOI 3) for 16 hours. ***$P < 0.001$ (One-way ANOVA with Dunnett's multiple comparison).

3.4 VSe1 and VSe1-28 Inhibit NFκB Activity

To further our understanding of how VSe1 and its analogues inhibit IFNβ production, we investigated the effects of VSe1 and VSe1-28 on the activity of key regulators of IFNβ expression. To do so, we treated 786-0 cells with VSe1 or VSe1-28, infected with VSVΔ51 for 8 hours and assessed the nuclear levels of NFκB p65, NFκB p50, IRF3 and c-jun by western blot. Interestingly, we found that the nuclear translocation of both the p65 and p50 subunits of NFκB were inhibited by VSe1 and VSe1-28, while the levels of IRF3 and c-jun in the nucleus remained unaffected (**Fig 8a**). This data was confirmed by testing the effects of both compounds on TNFα-induced nuclear translocation of NFκB p65. As expected, both VSe1 and VSe1-28 inhibited p65 translocation upon TNFα stimulation (**Fig 8b**). Given this interesting phenotype, we then proceeded to investigate the upstream regulation of NFκB activity by western blot in cells treated with VSe1 or VSe1-28 then stimulated with TNFα. We found that TNFα-induced phosphorylation of NFκB p65 and degradation of IκBα were unaffected by either compound (**Fig 9a**). Furthermore, virus-induced p65-p50 heterodimerization was still evident in presence of compounds (**Fig 9b**), suggesting that VSe1 and VSe1-28 hamper the nuclear translocation of p65 and p50 even though upstream signals from the IKK complex occur normally. Also, virus-induced phosphorylation of IRF3, c-jun and ATF2 was assessed and found to be unaffected by VSe1 and VSe1-28 (**Fig 9c**), confirming functional PRR signalling upon infection.

NFκB is a well-known inducer of IFNβ and other antiviral cytokines including IL-6 and TNFα. In order to determine if VSe1 and its analogues also impaired the production of these pro-inflammatory cytokines, we assessed their mRNA expression by RT-PCR. Consistent with our observations on IFNβ production, we found that VSe1 and VSe1-28 inhibited virus-induced mRNA expression of IL-6 and TNFα was for up to 24 hours or 16 hours post-infection respectively

(**Fig 10a & b**). These results were further validated by measuring the levels of TNFα secreted by the cells upon infection. As expected, both VSe1 and VSe1-28 inhibited the secretion of TNFα as measured by ELISA (**Fig 10c**). To test the functional relevance of NFκB inhibition as a potential mechanism of action, we tested a known inhibitor of NFκB, BAY 11-7085. This compound inhibits NFκB activation by inhibiting IKKs and preventing the phosphorylation and degradation of IκBα [139]. Interestingly, we found that BAY 11-7085 sensitized 786-0 cells to VSVΔ51 infection in a similar manner to VSe1 and VSe1-28 and enhanced virus production by 1000-fold (**Fig 11,** performed by Ramya Krishnan).

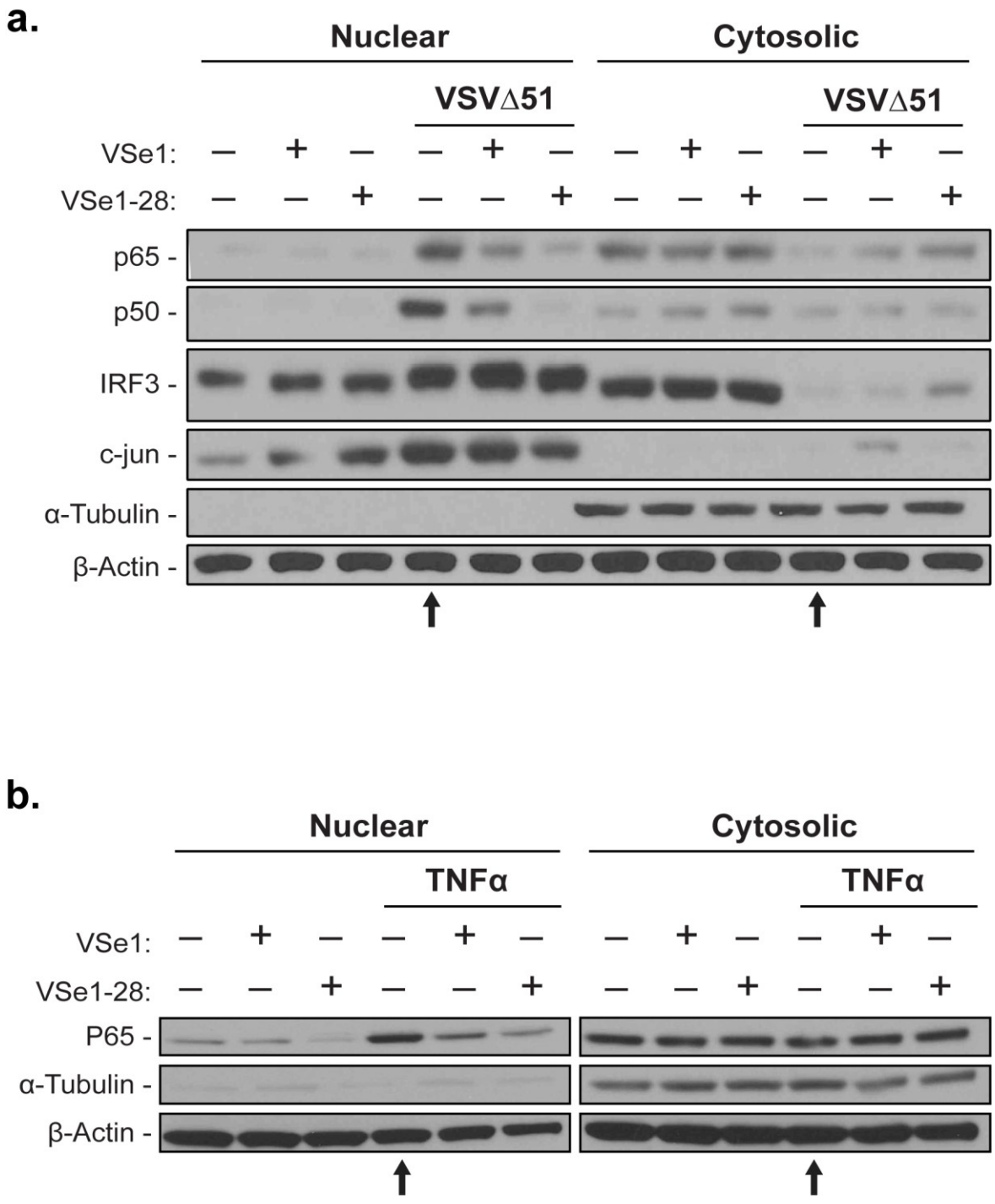
a.
Nuclear
Cytosolic
VSVΔ51
VSVΔ51
VSe1:
VSe1-28:
p65 -
p50 -
IRF3 -
c-jun -
α-Tubulin -
β-Actin -
b.
Nuclear
Cytosolic
TNFα
TNFα
VSe1:
VSe1-28:
P65 -
α-Tubulin -
β-Actin -

Figure 8. VSe1 and VSe1-28 inhibit the nuclear translocation of NFκB. (a) Western blot analysis on nuclear and cytosolic extracts from 786-0 cells treated with VSe1 (60 μM) or VSe1-28 (90 μM) then infected with VSVΔ51-GFP (MOI 1) for 8 hours. **(b)** Western blot analysis on nuclear and cytosolic extracts from 786-0 cells treated with VSe1 (60 μM) or VSe1-28 (90 μM) then infected with treated with TNFα (25 ng/mL) for 30 minutes. Arrows indicate VSVΔ51-infected control.

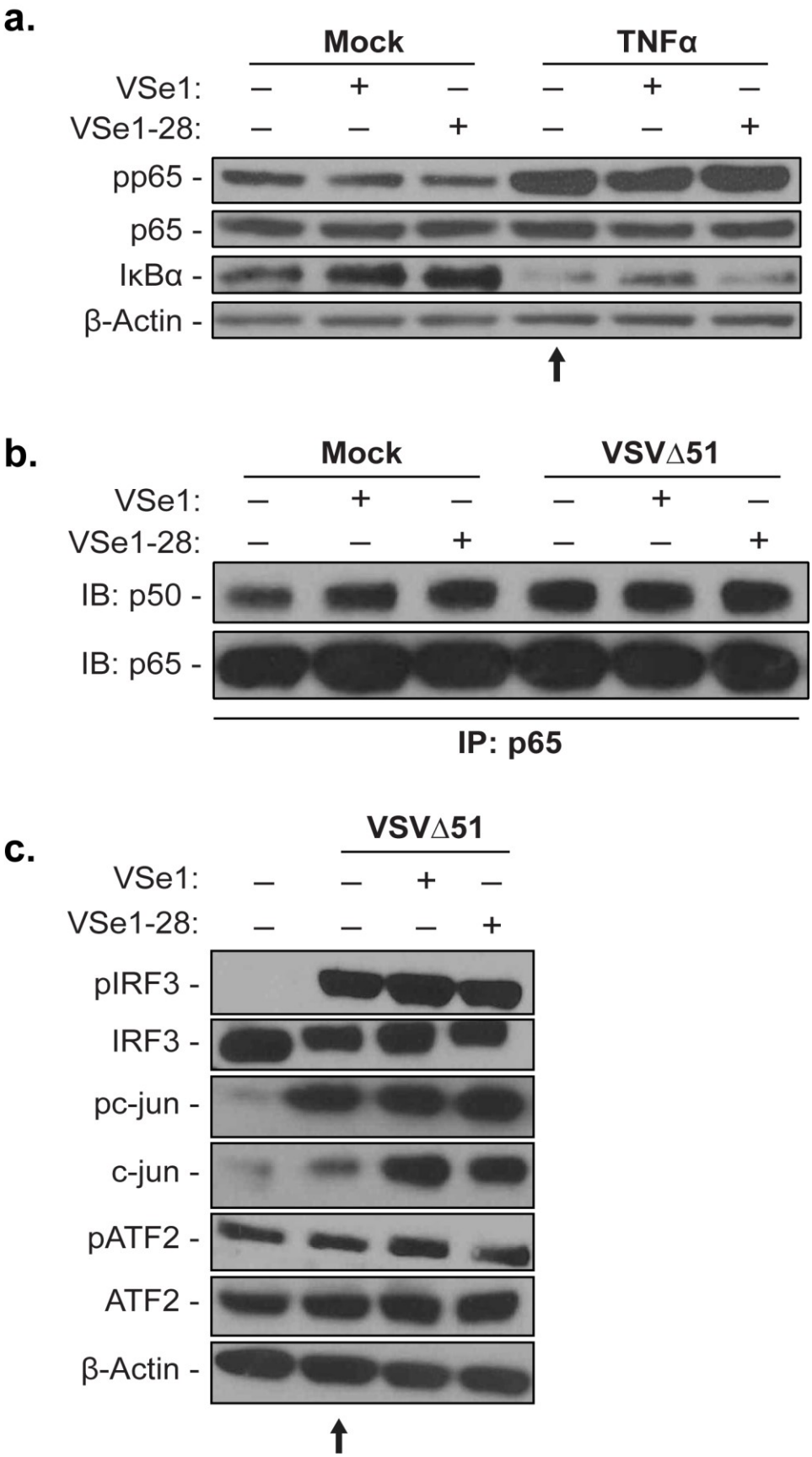
a.
Mock
TNFα
VSe1:
VSe1-28:
pp65 -
p65 -
IκBα -
β-Actin -
b.
Mock
VSVΔ51
VSe1:
VSe1-28:
IB: p50 -
IB: p65 -
IP: p65
c.
VSVΔ51
VSe1:
VSe1-28:
pIRF3 -
IRF3 -
pc-jun -
c-jun -
pATF2 -
ATF2 -
β-Actin -

Figure 9. VSe1 and VSe1-28 do not effect NFκB p65 phosphorylation or dimerization with p50. (a) Western blot analysis using whole cell lysates from 786-0 cells treated with VSe1 (60 μM) or VSe1-28 (90 μM) then treated with TNFα (25 ng/mL) for 30 minutes. **(b)** NFκB p65 was immunoprecipitated from lysates from 786-0 cells treated with VSe1 (60 μM) or VSe1-28 (90 μM) then infected with VSVΔ51-GFP (MOI 1) for 8. Proteins were separated by SDS-PAGE then probed for NFκB p50. **(c)** Whole cell lysates from **b** were used to analyze the phosphorylation status of IRF3, c-jun and ATF2 by western blot.

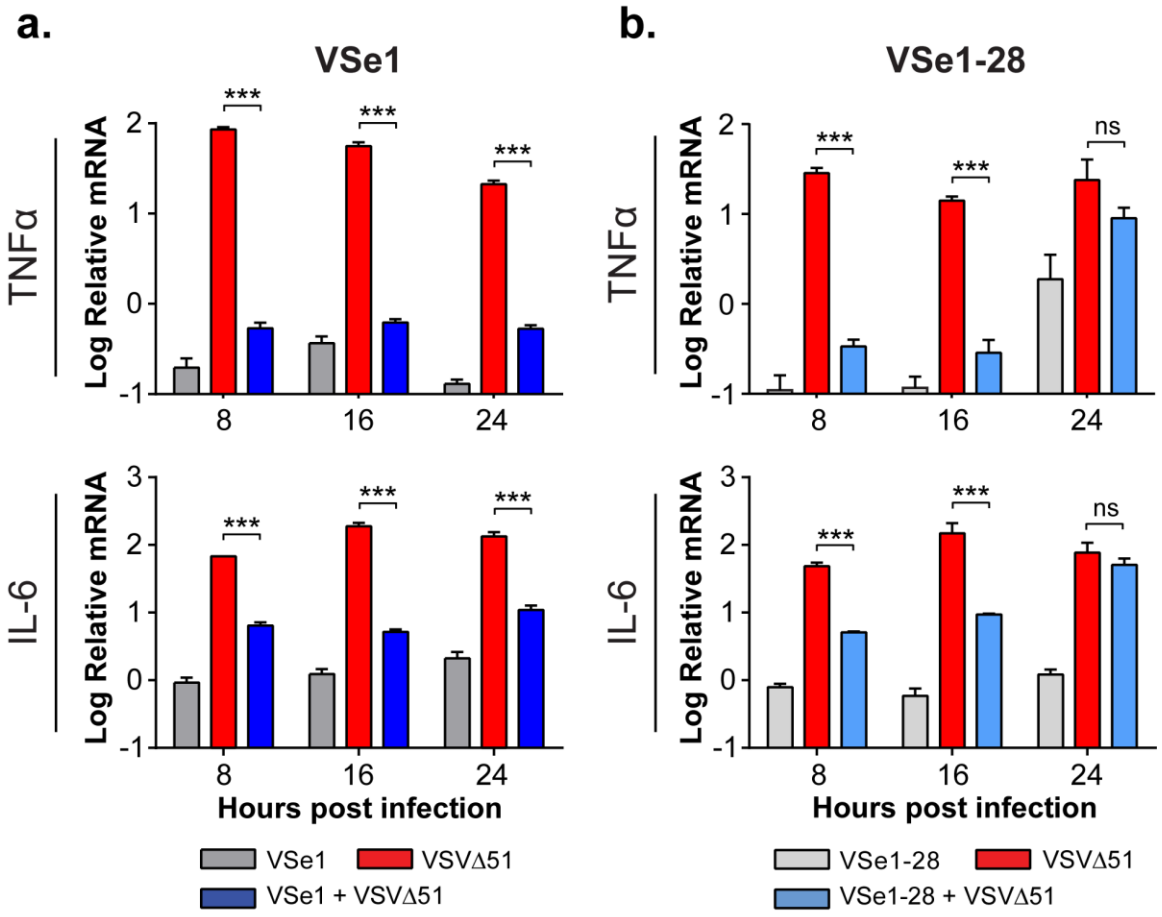
a.
VSe1
TNFα
IL-6
Log Relative mRNA
***
8
16
24
Hours post infection
VSe1
VSVΔ51
VSe1 + VSVΔ51
b.
VSe1-28
ns
VSe1-28
VSe1-28 + VSVΔ51

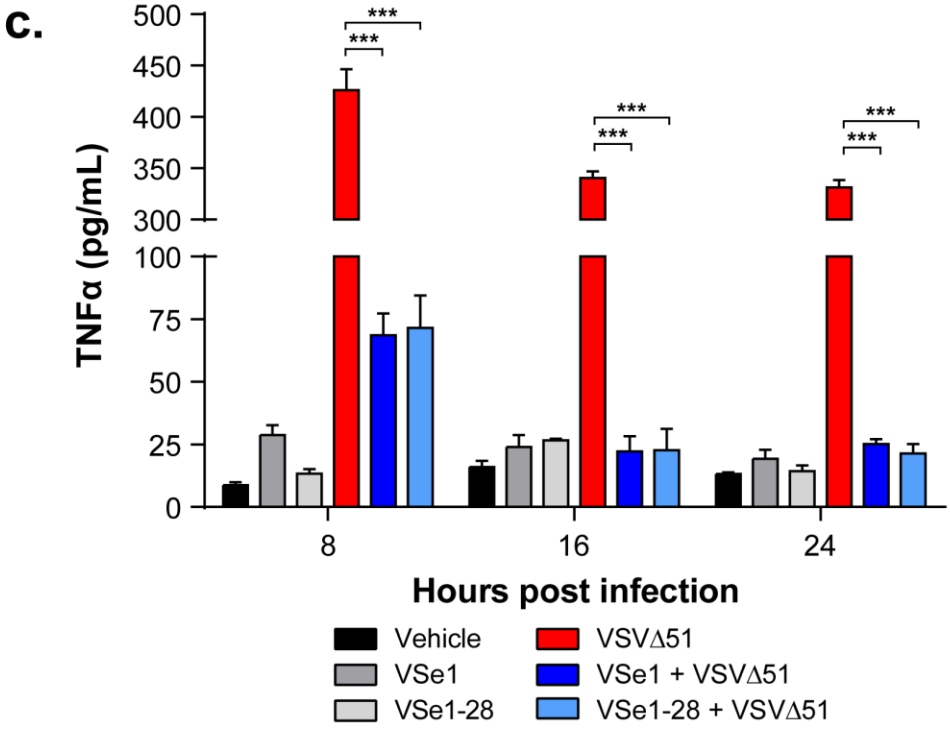
c.
TNFα (pg/mL)
500
450
400
350
300
100
75
50
25
0
***
8
16
24
Hours post infection
Vehicle
VSe1
VSe1-28
VSVΔ51
VSe1 + VSVΔ51
VSe1-28 + VSVΔ51

Figure 10. VSe1 and VSe1-28 inhibit the expression of NFκB target genes. Quantitative RT-PCR analysis using RNA from 786-0 cells treated with **(a)** VSe1 (60 μM) or **(b)** VSe1-28 (90 μM) then infected with VSVΔ51 (MOI 1). RNA was extracted 8, 16 and 24 hours post-infection and the expression of TNFα and IL-6 were determined. **(c)** TNFα production was measured by ELISA using supernatants from **a** and **b**. ns: $P > 0.05$, ***$P < 0.001$ (Two-way ANOVA with Dunnett's multiple comparison).

a.

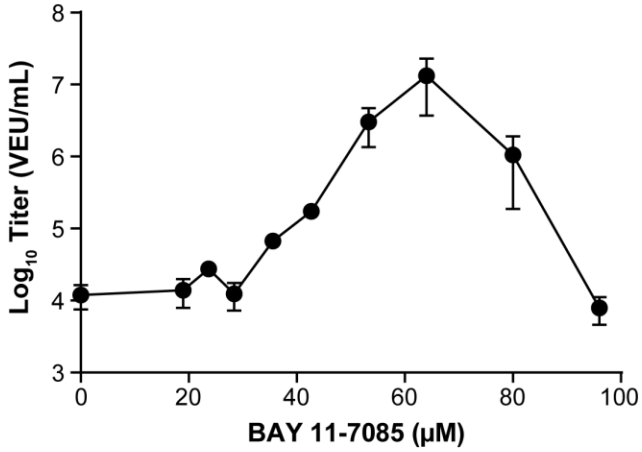
Log10 Titer (VEU/mL)
8
7
6
5
4
3
0
20
40
60
80
100
BAY 11-7085 (μM)

b.

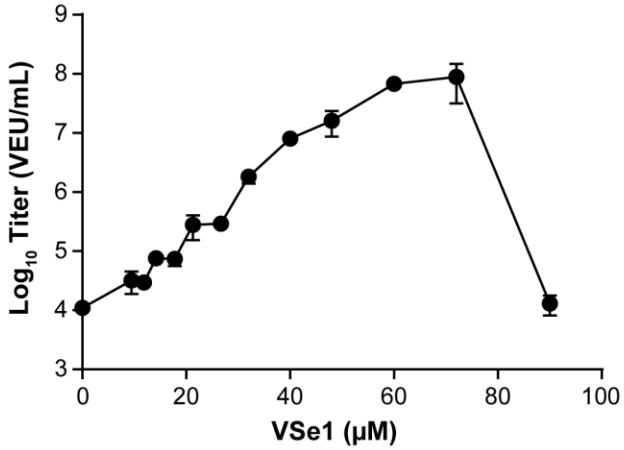
Log10 Titer (VEU/mL)
9
8
7
6
5
4
3
0
20
40
60
80
100
VSe1 (μM)

c.

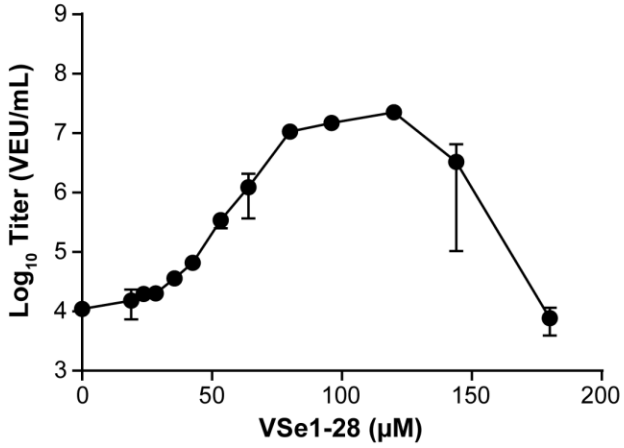
Log10 Titer (VEU/mL)
9
8
7
6
5
4
3
0
50
100
150
200
VSe1-28 (μM)

Figure 11. BAY 11-7085 sensitizes 786-0 cells to oncolytic viral infection. 786-0 cells were pre-treated with **(a)** BAY 11-7085, **(b)** VSe1 (60 μM) **(c)** VSe1-28 (90 μM) then infected with VSVΔ51-Fluc (MOI 0.005). Supernatants were collected 40 hours later and virus output was determined using a previously described luciferase-based titration assay [134]. This data was generated by Ramya Krishnan.

3.4 VSe1 and VSe1-28 Deplete Cellular GSH Levels

We have previously demonstrated that VSe1 and analogs react with free glutathione [108] and have generated data showing that VSe1 and VSe1-28 inhibit the activity of multiple GSTs, including GSTP1 with an IC_{50} of 2.67μM for VSe1 (data not shown). We considered it possible that these properties could play a role in the observed inhibitory effects of VSe1 and VSe1-28 on NFκB nuclear translocation. To further characterize the effects of VSe1 and VSe1-28 on glutathione homeostasis, 786-0 cells were treated with either compound then the levels of reduced and oxidized glutathione were measured by HPLC-UV detection at different time points. We found that GSH levels were depleted after 1 hour of treatment then robustly increased 12 hours post-treatment (**Fig 12**). Interestingly, VSe1-28 caused a greater depletion of cellular GSH that lasted for at least 4 hours, unlike its parent compound VSe1, for which the levels were already higher than baseline at 4 hours post-treatment (**Fig 12**). It has been demonstrated that cinnamaldehyde, an electrophile containing an α,β-unsaturated carbonyl similar to VSe1 and VSe1-28, causes a short-term depletion in GSH levels followed by increased intracellular levels of GSH and GRX-1 in the long term, a pattern that is similar to the one we observed. This in turn was found to correlate with increased glutathionylation of the p65 subunit of NFκB and decreased NFκB activity and nuclear translocation [130]. To assess the involvement GSH homeostasis in anti-viral protection, we tested cinnamaldehyde's effect on VSVΔ51 replication in 786-0 cells and found that it enhanced virus replication and increased virus-mediated cytotoxicity (**Fig 13**). While this supports a broader impact of compounds with α,β-unsaturated carbonyls on the anti-viral response, it does not establish a role for glutathionylation in mediating this effect. To investigate this more directly in our system, we assessed the effect of VSe1 and VSe1-28 on p65 glutathionylation by treating cells prior to p65 immunoprecipitation. Glutathionylation was then measured by western blot using an anti-GSH

antibody under non-reducing conditions (**Fig 14a**). As a positive control, lysates were treated with 50 mM of oxidized glutathione (GSSG) to induce protein glutathionylation (**lane 6, fig 14a**). Our results show the complete absence of p65 glutathionylation with and without VSe1 and VSe1-28. Furthermore, we tested the effect of VSe1 and VSe1-28 on cells depleted of cellular GSH. To do so, 786-0 cells were cultured in BSO for 6-10 days to inhibit the synthesis of GSH. Upon verifying that intracellular GSH was depleted by HPLC (**Fig 14b,** performed by Ramya Krishnan), BSO cultured cells were pre-treated with VSe1 or VSe1-28 then infected with VSVΔ51. Interestingly, we found that the potency of VSe1 and VSe1-28 increased upon complete depletion of GSH (**Fig 14c**).

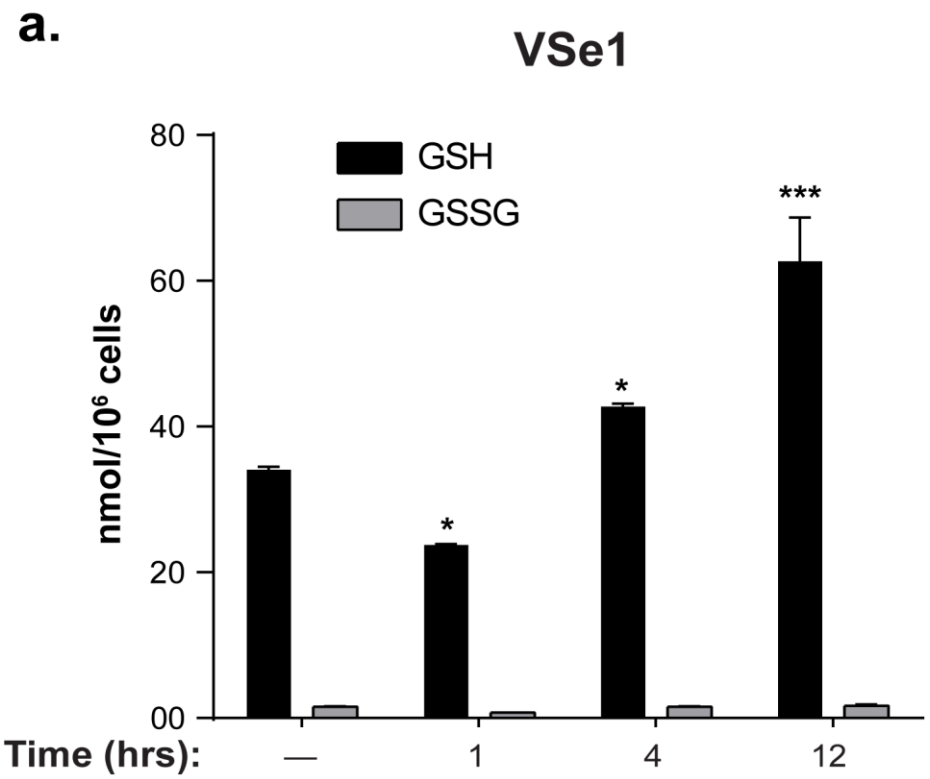
a.
VSe1
GSH
GSSG
nmol/10^6 cells
80
60
40
20
00
*
*
***
Time (hrs):
—
1
4
12

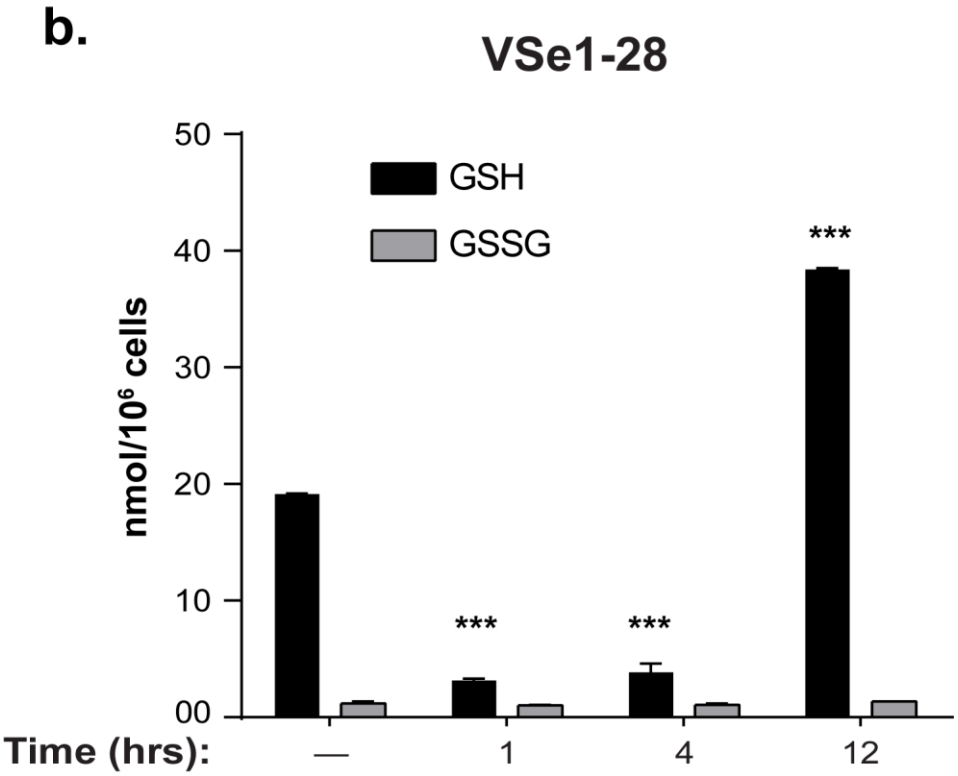
b.
VSe1-28
GSH
GSSG
nmol/10^6 cells
50
40
30
20
10
00
***
***
***
Time (hrs):
—
1
4
12

Figure 12. VSe1 and VSe1-28 deplete cellular GSH. Cellular GSH and GSSG levels were measured by HPLC-UV detection using whole cell lysates from 786-0 cells treated with (a) VSe1 (60 μM) or (b) VSe1-28 (90 μM) for 1, 4, and 12 hours.

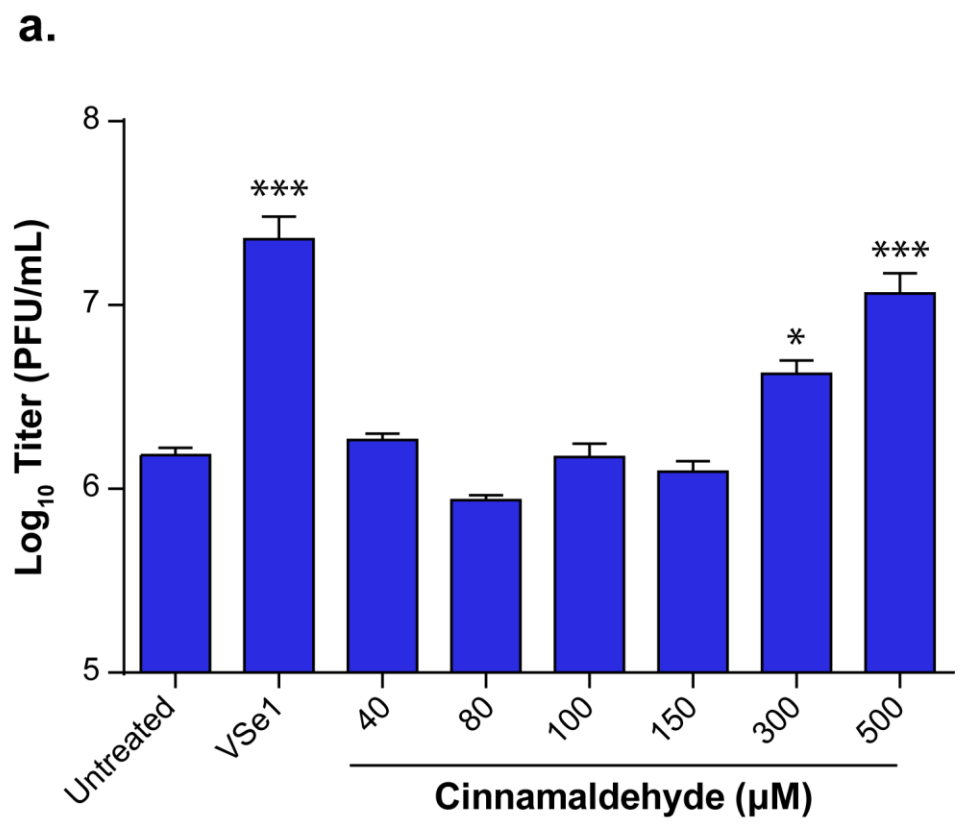
a.
8
7
6
5
Log10 Titer (PFU/mL)
***
*
***
Untreated
VSe1
40
80
100
150
300
500
Cinnamaldehyde (μM)

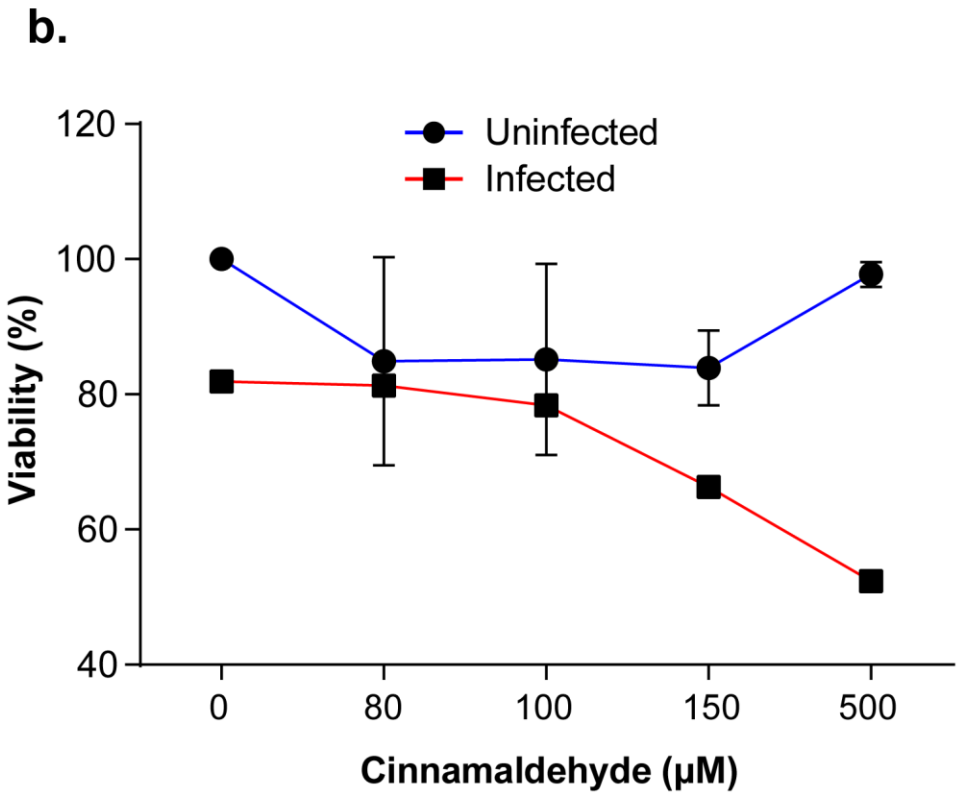
b.
120
100
80
60
40
Viability (%)
Uninfected
Infected
0
80
100
150
500
Cinnamaldehyde (μM)

Figure 13. Cinnamaldehyde potentiates VSVΔ51 infection and cytotoxicity. 786-0 cells were treated with increasing doses of cinnamaldehyde then infected with VSVΔ51 (MOI 0.01). **(a)** Virus output and **(b)** cell viability were measured 40 hours post infection by plaque assay and AlamarBlue respectively.

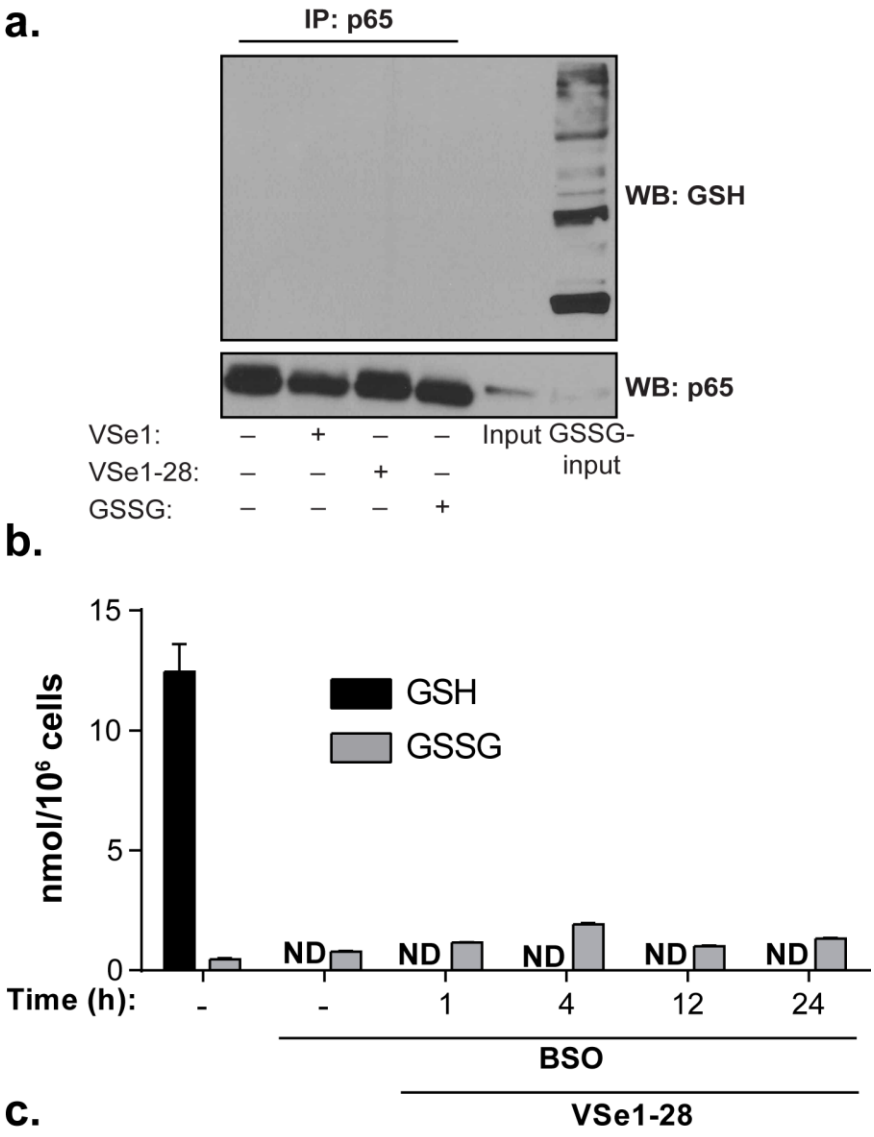
a.
IP: p65
WB: GSH
WB: p65
VSe1: – + – – Input GSSG-input
VSe1-28: – – + –
GSSG: – – – +
b.
nmol/10⁶ cells
15
10
5
0
GSH
GSSG
ND
ND
ND
ND
ND
Time (h): - - 1 4 12 24
BSO
VSe1-28
c.
Log₁₀ Titer (VEU/mL)
8
7
6
5
4
3
2
0 20 40 60 80 100 120
Concentration (μM)
VSe1
VSe1 + BSO
VSe1-28
VSe1-28 + BSO

Figure 14. VSe1 and VSe1-28 do not induce NFκB p65 glutathionylation. (a) p65 was immunoprecipitated using lysates from 786-0 cells treated with VSe1 (60 μM) or VSe1-28 (90 μM) for 12 hours. p65 glutathionylation status was assessed by western blot. As a positive control, lysates were treated with 50mM GSSG for 30 minutes to induce protein glutathionylation. **(b)** Cellular GSH and GSSG levels were measured by HPLC-UV detection using whole cell lysates from 786-0 cells cultured in DMEM supplemented with BSO (2mM) for 10 days then treated with VSe1-28 for the indicated times. ND: not detectable **(c)** Virus titers measured by luciferase-based titration assay using supernatants from 786-0 cells cultured in DMEM supplemented with BSO (2mM) for 10 days then treated with VSe1 or VSe1-28 prior to infection with VSVΔ51-Fluc (MOI 0.005) for 40 hours. The data for c was generated by Ramya Krishnan.

3.5 VSe1 and VSe1-28 Induce Oxidative Stress

Since GSH and GSTs are key regulators of cellular redox homeostasis, we considered whether the simultaneous impact of VSe1 or VSe1-28 on GSH levels and GST activity could cause a shift in cellular redox state, indirectly leading to dysregulation of NFκB activity. To further assess the effect of VSe1 and VSe1-28 on cellular redox state, the microarray data from section **3.1** was used to analyze the expression of genes involved in the anti-oxidant response. We found that all the active analogues of VSe1 highly upregulated genes responding to oxidative stress, albeit less substantially for pyrrole analogues (**Fig 15**). For example, heme oxygenase 1 (HMOX1) was consistently upregulated in all active, but not inactive compounds. The kinetics of this upregulation was further assessed by quantitative RT-PCR using RNA from cells treated with VSe1 or VSe1-28 prior to VSVΔ51 infection. In line with the microarray data, HMOX-1 and OSGIN (oxidative stress induced growth inhibitor) were highly upregulated by both VSe1 and VSe1-28, even in absence of infection (**Fig 16**). Interestingly, HMOX-1 was maximally induced 8h post-treatment with VSe1 and VSe1-28 alone.

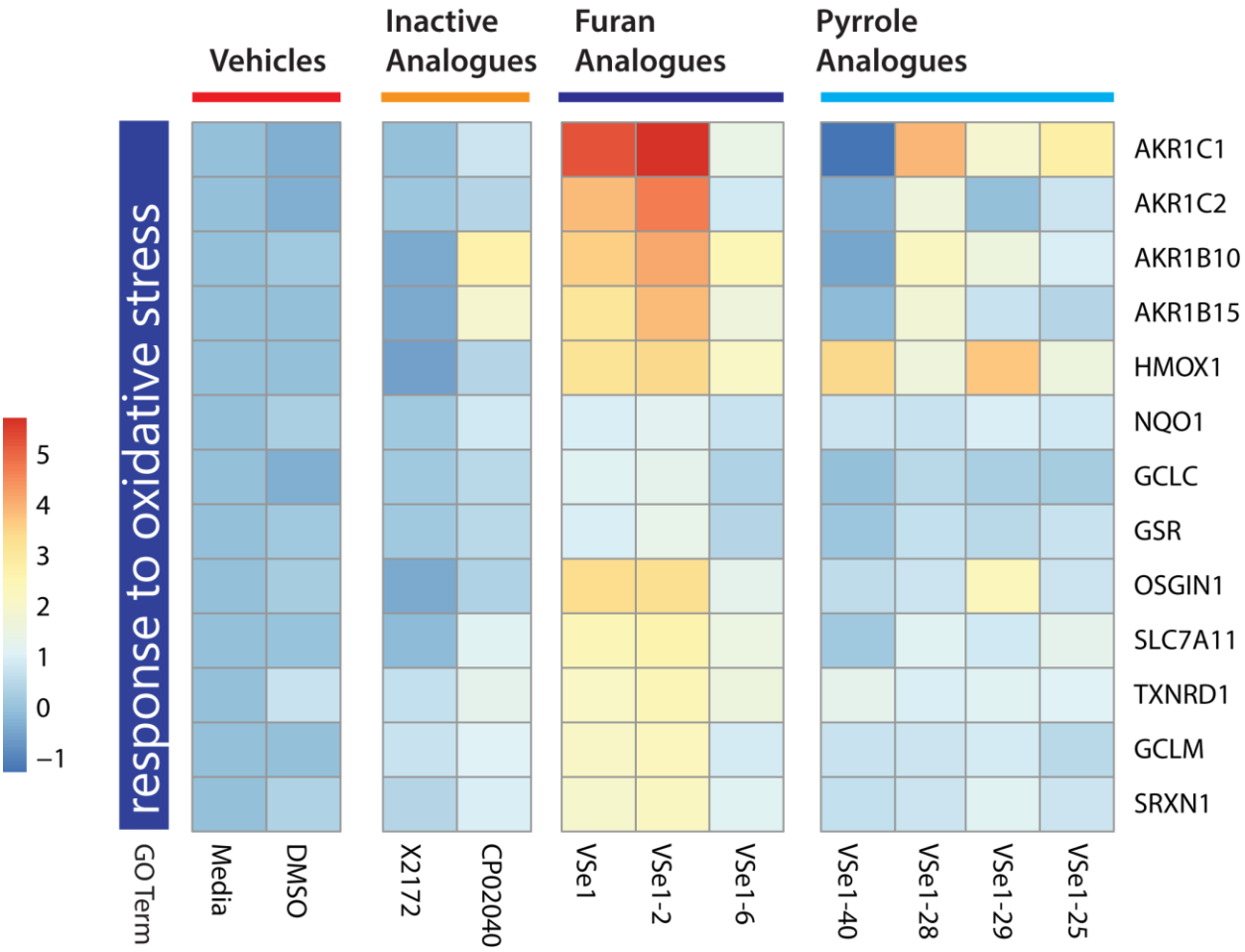
Vehicles
Inactive Analogues
Furan Analogues
Pyrrole Analogues
response to oxidative stress
5
4
3
2
1
0
−1
AKR1C1
AKR1C2
AKR1B10
AKR1B15
HMOX1
NQO1
GCLC
GSR
OSGIN1
SLC7A11
TXNRD1
GCLM
SRXN1
GO Term
Media
DMSO
X2172
CP02040
VSe1
VSe1-2
VSe1-6
VSe1-40
VSe1-28
VSe1-29
VSe1-25

Figure 15. VSe1 and its analogues upregulate genes that respond to oxidative stress. Micro-array analysis using RNA from 786-0 cells treated with media, vehicle (DMSO), or viral sensitizer for 24 hours. Triplicates were pooled and hybridized on Affymetrix Human PrimeView Array. Shown are heat maps of genes contained within the GO term “Response to Oxidative Stress”.

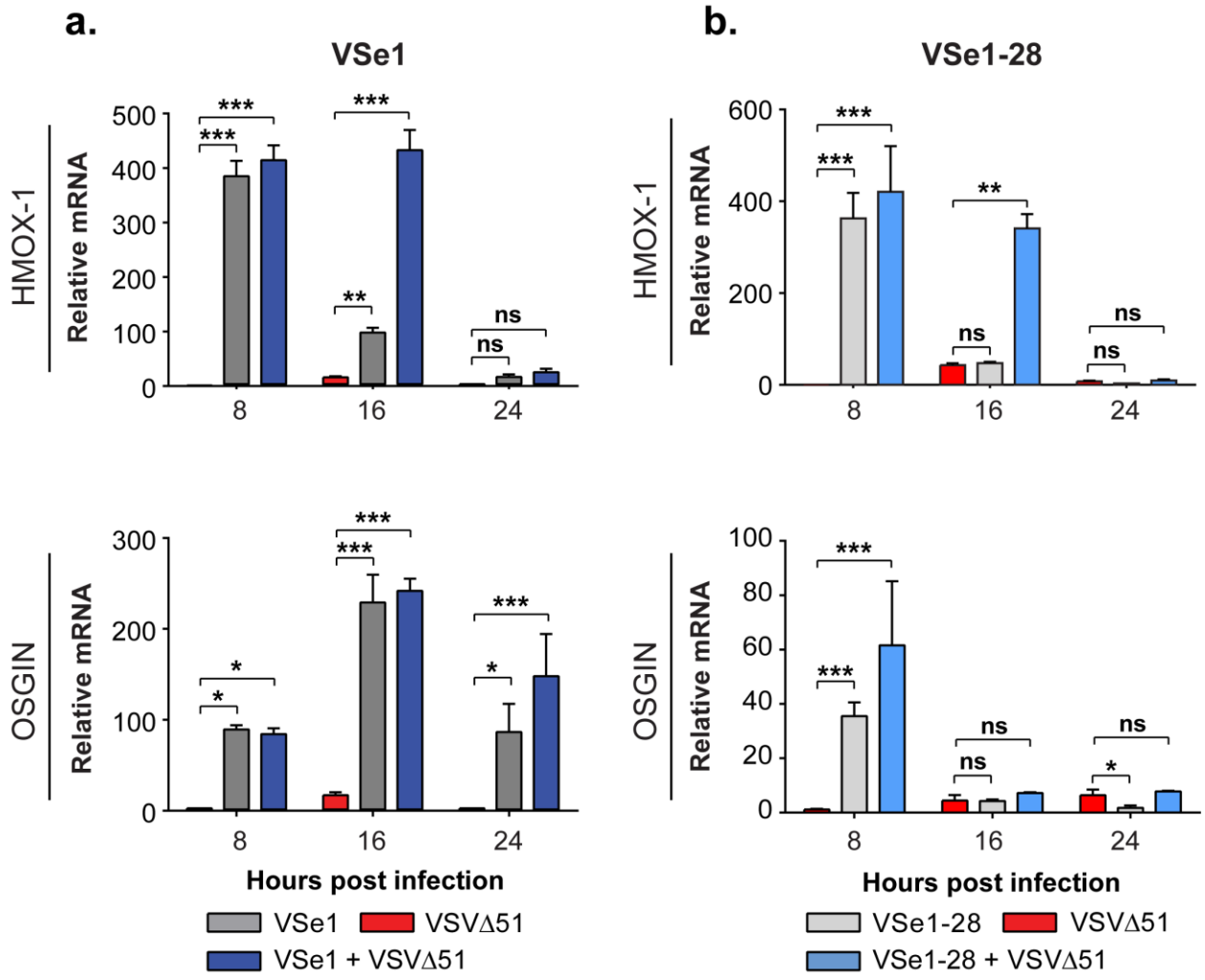
a.
VSe1
HMOX-1
Relative mRNA
500
400
300
200
100
0
***
***
***
**
ns
ns
8
16
24
OSGIN
Relative mRNA
300
200
100
0
*
*
***
***
*
***
8
16
24
Hours post infection
VSe1
VSVΔ51
VSe1 + VSVΔ51
b.
VSe1-28
HMOX-1
Relative mRNA
600
400
200
0
***
***
**
ns
ns
ns
8
16
24
OSGIN
Relative mRNA
100
80
60
40
20
0
***
***
ns
ns
ns
*
8
16
24
Hours post infection
VSe1-28
VSVΔ51
VSe1-28 + VSVΔ51

Figure 16. VSe1 and VSe1-28 upregulate HMOX1 and OSGIN. Quantitative RT-PCR analysis using RNA from 786-0 cells treated with **(a)** VSe1 (60 μM) or **(b)** VSe1-28 (90 μM) then infected with VSVΔ51 (MOI 1). RNA was extracted 8, 16 and 24 hours post-infection and the expression of HMOX1 and OSGIN were determined. ns: $P > 0.05$, *$P < 0.05$, **$P < 0.01$, ***$P < 0.001$ (Two-way ANOVA with Dunnett's multiple comparison).

3.6 H_2O_2 Enhances VSVΔ51 Infection and Inhibits NFκB Activity

Our data altogether suggested that VSe1 and its structural analogues might impair NFκB activity indirectly through the formation of ROS intermediates. Indeed, NFκB subunits are known to contain redox-sensitive cysteines that can regulate NFκB activity depending on their oxidation state [140]. To assess the interplay between oxidative stress and sensitization to viral infection, 786-0 cells were treated with increasing concentrations of hydrogen peroxide (H_2O_2) prior to VSVΔ51 infection. Interestingly, H_2O_2 was found to enhance virus output in a dose-dependant manner at final concentrations ranging from 1 to 6 mM (**Fig 17**). We then tested the effects of H_2O_2 on NFκB activity and found that H_2O_2 also inhibited virus-induced nuclear translocation of NFκB p65 and p50 in a dose-dependant manner (**Fig 18a**). We further validated this observation by assessing the induction of genes downstream of NFκB, namely IFNβ, TNFα and IL-6. Interestingly, virus-induced expression of IFNβ was robustly inhibited by all doses of H_2O_2 (**Fig 18b**), including doses that had little impact on VSVΔ51 infection (Fig 17). On the other hand, TNFα and IL-6 expression (**Fig 18c and d**) were inhibited in a dose-dependant manner that resembles the trend seen with virus output (**Fig 17**) and NFκB nuclear translocation (**Fig 18a**). Finally, primers for VSV M were also used to confirm active infection in these cells (**Fig 18e**). Altogether this data suggests that oxidative stress can enhance VSVΔ51 infection by impairing cytokine production through dysregulation of NFκB activity.

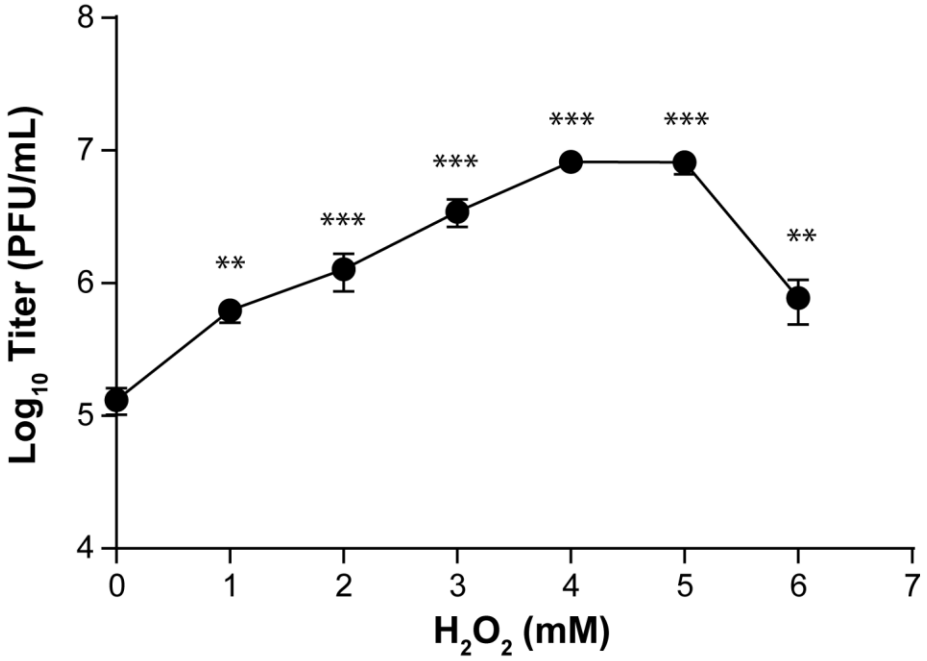
8
7
6
5
4
0
1
2
3
4
5
6
7
Log10 Titer (PFU/mL)
H2O2 (mM)
**
***
***
***
***
**

Figure 17. H_2O_2 potentiates VSVΔ51 infection in a dose-dependant manner. Virus titers were determined by plaque assay using supernatants from 786-0 cells treated with increasing doses H_2O_2 then infected with VSVΔ51 (MOI 0.01) for 40 hours. **P < 0.01, ***P < 0.001 (One-way ANOVA with Dunnett's multiple comparison).

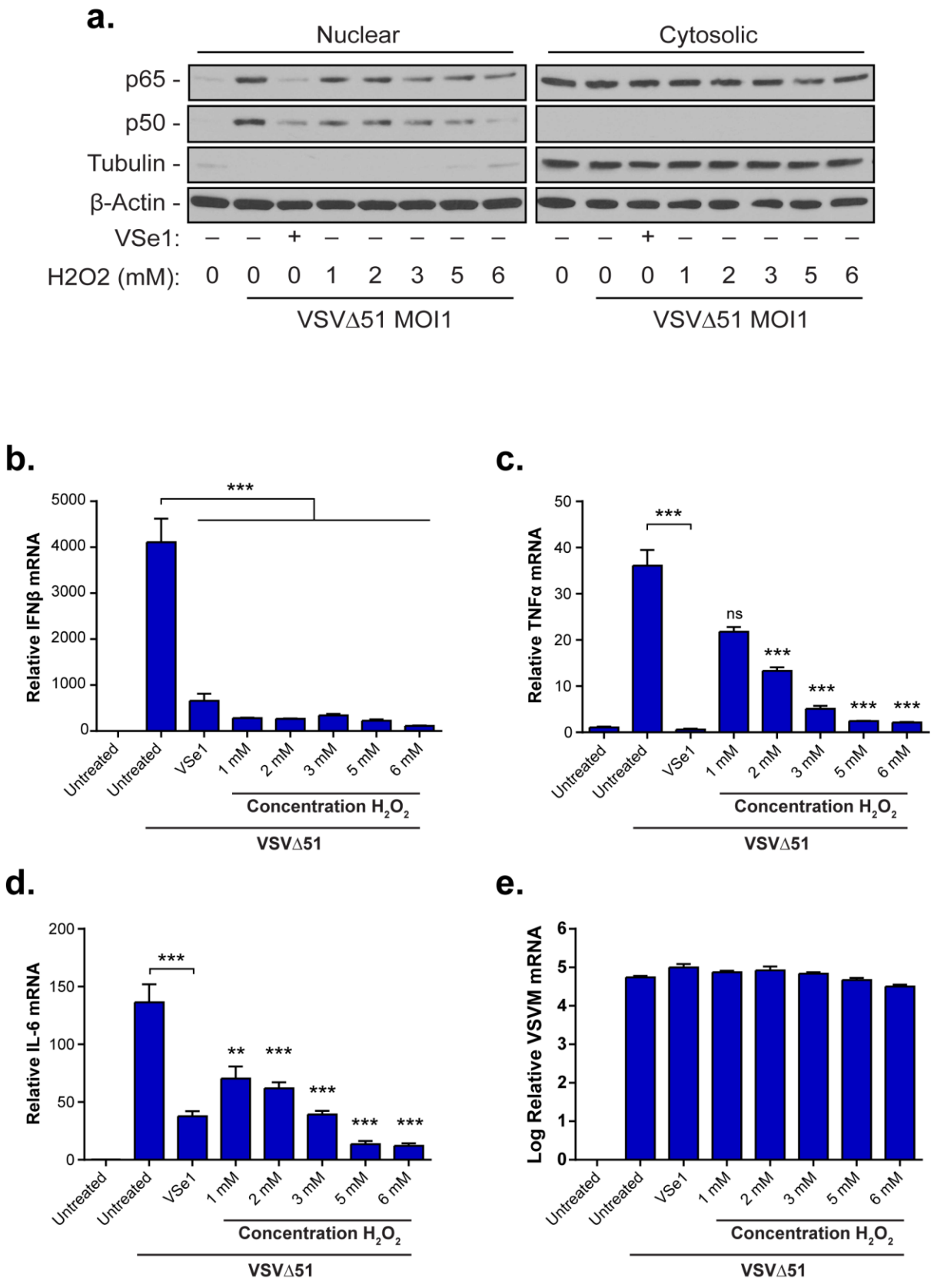
a.
Nuclear
Cytosolic
p65 -
p50 -
Tubulin -
β-Actin -
VSe1: – – + – – – – – – – + – – – – –
H2O2 (mM): 0 0 0 1 2 3 5 6 0 0 0 1 2 3 5 6
VSVΔ51 MOI1
VSVΔ51 MOI1
b.
Relative IFNβ mRNA
5000
4000
3000
2000
1000
0
***
Untreated
Untreated
VSe1
1 mM
2 mM
3 mM
5 mM
6 mM
Concentration H2O2
VSVΔ51
c.
Relative TNFα mRNA
50
40
30
20
10
0
***
ns
***
***
***
***
Untreated
Untreated
VSe1
1 mM
2 mM
3 mM
5 mM
6 mM
Concentration H2O2
VSVΔ51
d.
Relative IL-6 mRNA
200
150
100
50
0
***
**
***
***
***
***
Untreated
Untreated
VSe1
1 mM
2 mM
3 mM
5 mM
6 mM
Concentration H2O2
VSVΔ51
e.
Log Relative VSVM mRNA
6
5
4
3
2
1
0
Untreated
Untreated
VSe1
1 mM
2 mM
3 mM
5 mM
6 mM
Concentration H2O2
VSVΔ51

Figure 18. H_2O_2 inhibits nuclear translocation and transcriptional activity of NFκB. 786-0 **c**ells were treated with increasing doses H_2O_2 then infected with VSVΔ51 (MOI 1). **(a)** Western blot analysis using nuclear and cytosolic extracts collected 8 hours post-infection. Quantitative RT-PCR for **(b)** IFNβ, **(c)** TNFα, **(d)** IL-6 and **(e)** VSV M expression using RNA extracted 16 hours post-infection. ns: $P > 0.05$, $^{**}P < 0.01$, $^{***}P < 0.001$ (Two-way ANOVA with Dunnett's multiple comparison).

4. Discussion

4.1 Enhancing VSVΔ51 Infection by Blocking the IFN Response

It is well known that VSV is an IFN-sensitive virus, and that the attenuated VSVΔ51 is even more dependant on defective IFN pathways of cancer cells to readily infect and kill them [47]. With the objective of increasing the sensitivity of resistant cancer cells to VSVΔ51, various groups have investigated several strategies to temporarily block the type I IFN response. For example, it has been demonstrated that JAK1 inhibitors can be used to enhance VSVΔ51 infection of resistant human melanoma and sarcoma models [141,142]. Based on this as well as previously published data, we initially hypothesized that VSe1 and its analogues also inhibit the response to type I IFNs [107,108]. Protection assays with IFNβ (**Fig 3**) revealed that VSe1 and its analogues may indeed hinder the antiviral effects of exogenous IFNβ. However, more experiments are required to determine if the enhancement seen is a result of suppressing the response to IFNβ through ISGF3 (STAT1/2 and IRF9) or through co-regulatory factors such as NF-κB. This could be done by repeating the protection assay (**Fig 3**) in cells with STAT1/2 or IRF9 knockdowns. If the VSes already inhibit the response to IFNβ then there will be no further enhancement of virus titers in STAT1/2-/- or IRF9-/- cells co-treated with IFNβ and VSes. Interestingly, our microarray and quantitative RT-PCR data (**Fig 4 & 5**) show that ISG induction upon type I IFN stimulation are supressed to different levels by all active VSes. Most notably, inhibition of ISG expression by VSe1 (furan) lasts longer than the inhibition by VSe1-28 (pyrrole) (**Fig 5**). It is unclear whether this difference is similar among other furan and pyrrole analogues, however this could easily be determined by analyzing the kinetics of ISG inhibition by qPCR with VSe1-2 (furan) and VSe1-10 (pyrrole).

Given that all the tested VSes could efficiently inhibit ISG expression and that the JAK-STAT pathway is upstream of these genes, the phosphorylation status of STAT1 was assessed (**Fig**

6). Western blots revealed that the furan VSes (VSe1 and VSe1-2) inhibits STAT1 phosphorylation upon IFNβ stimulation. Therefore, we propose that the inhibition occurs within the first 2 hours of pre-treatment, since lysates are collected 30 minutes post-IFNβ stimulation after a 2-hour pre-treatment period with VSes. This observation is in line with previously published data that shows the furan compounds are more reactive than the pyrrole analogues [108]. Since ISGs are inhibited by all compounds, but we observe an inhibition of STAT1 phosphorylation by furan VSes alone, our data suggests that the viral sensitizing properties of our compounds do not depend on this pathway. Despite these findings, it still remains possible that the VSes inhibit other components of JAK-STAT signalling. To fully characterize the effect of the compounds on this pathway, we could assess the phosphorylation status of JAK1, TYK2 and IRF9 as well as: 1. the nuclear translocation (immunofluorescence and western blot on fractionated lysates), 2. the dimerization (immunoprecipitation) and 3. the DNA-binding activity (EMSA or ChIP PCR) of STAT1 and 2. Interestingly, inhibition of the JAK-STAT pathway may not be essential for the prevention of ISG expression. Despite being rarely described, JAK-STAT-independent regulation of ISG expression has been documented. Indeed, NFκB has been shown to regulate the expression of ISGs and can also be activated by type I IFNs [143]. Therefore, the inhibition of NFκB activity by the VSes could explain their suppressive effects on ISG expression.

4.2 VSe1 and VSe1-28 Inhibit NFκB Activity

Based on the data presented, we propose that the inhibition of ISG expression by VSe1 and VSe1-28 is a result of their inhibition of NFκB nuclear translocation (**Fig 8a**). Our results show that the compounds inhibit both virus and TNFα-mediated NFκB nuclear translocation and that this inhibition occurs within 2.5 hours of drug treatment and last for up to 10 hours (**Fig 8**), which is in line with the inhibition of cytokine production that is observed as early as 8 hours post-

infection (**Fig 7 & 10**). Interestingly, single and multi-step viral growth curves performed by another lab member demonstrate that both VSe1 and VSe1-28 increase the production of VSVΔ51 as early as 8 hours (data not shown). While this kinetic suggests that inhibition of NFκB activity by the VSes can prevent cytokine production by infected cells and sensitize them to infection, this possibility needs to be validated further. Importantly, we continue to demonstrate that the compound BAY 11-7085, an inhibitor of the NκFB pathway via inhibition of IκBα phosphorylation, was able to sensitize cells to VSVΔ51 (**Fig 11**). To evaluate the importance of NFκB inhibition for the viral sensitizing activity of our compounds, we could test our inactive analogues for their effect on NFκB activity and cytokine production. We would expect the inactive analogues to have no impact on NFκB activity (phosphorylation status and nuclear translocation). Furthermore, we should find that cytokine production (ELISA and RT-PCR) is still active in the presence of the inactive analogues. Altogether, these data would suggest that our active VSes inhibit the nuclear translocation of NFκB and its transcriptional activity, which in turn would decrease the virus-induced production of IFNβ, TNFα and IL-6, and enhance VSVΔ51 propagation in cancer cells but not in normal cells.

As a result of its anti-apoptotic activity, NFκB is often associated with resistance to anti-cancer drugs. Because of this property, NFκB inhibitors have been fiercely pursued with the objective of using them in combination with existing anti-cancer agents [144]. Most NFκB inhibitors consist of protein kinase antagonists that prevent the phosphorylation of NFκB and IκBα, proteasome/ubiquitination inhibitors that prevent the degradation of IκBα, or phosphatase agonists that induce dephosphorylation of NFκB, and therefore act upstream of nuclear translocation. Because of their broad roles, these NFκB inhibitors are rarely specific and will often affect other signalling pathways, which raises concern when it comes to off-tissue effects and toxicity [145].

Indeed, even inhibitors of NFκB nuclear translocation are often antagonist of importins, and so inhibit the translocation of other transcription factors [146]. Notably, NFκB and IRF3 are shuttled into the nucleus by the same importins [146] and our data demonstrates that IRF3 nuclear translocation is still functional with VSe1 and VSe1-28 (**Fig 8a**). Therefore, our VSe compounds do not likely inhibit importin activity. Furthermore, upstream IKK signalling is functional as demonstrated by consistent IκB degradation (**Fig 9a**) and p65-p50 dimerization (**Fig 9b**). Since pyrrole-based VSes inhibit NFκB at the level of nuclear translocation, they could be tested in combination with other anti-cancer drugs, radiotherapy, or even in triple combinations with anti-cancer drugs and OVs to maximize virus-induced apoptosis of tumour cells.

We have yet to determine the effects of our viral sensitizers on the non-canonical NFκB pathway. This can easily be determined by assessing p100 degradation and the nuclear translocation of p52 and RelB. Like other subunits of the κB family, p52 and RelB are regulated by many post-translational modifications including phosphorylation [147,148], polyubiquitination [149], SUMOylation [149], and acetylation [150,151], however redox-mediated regulation of either subunit has not been reported. Indeed, it would be interesting to investigate the effects of the viral sensitizers on the non-canonical NFκB pathway given its role in lymphocyte development.

4.3 VSe1 and VSe1-28 Inhibit Cytokine Production

While the VSes differ in their effects on the JAK-STAT pathway, we found that all of them could robustly inhibit the production of IFNβ (**Fig 7c**). We chose one furan (VSe1) and one pyrrole (VSe1-28) to further characterize their effects on cytokine production and found that both analogues could also inhibit the production of TNFα and IL-6 (**Fig 10**). Interestingly, inhibition of both TNFα and IFNβ could explain the selectivity of our compounds to cancer cells. Indeed, TNFα has been shown to synergize with IFNβ to protect normal fibroblasts against viral infection, a

phenomenon that was not evident in cancer cells [152]. Given that both cytokines are inhibited by VSe1 and VSe1-28, this may partially explain the cancer-selective effects of the VSes, since even low levels of the two cytokines should be sufficient to synergize and could explain why normal cells remain protected but not cancer cells. Although the inhibition of antiviral cytokine production is in line with the viral sensitizing properties of the VSes, we still haven't proven that the two phenomena are linked. To investigate this, we could use virus-conditioned media instead of direct virus infection or treatment with IFNβ only. Virus-conditioned media should contain the antiviral cytokines produced by infected cells and protect the fresh cells from VSVΔ51 infection, while conditioned media from cells pre-treated with VSes and then infected should contain less cytokines and so should not protect the cells from VSVΔ51 infection as effectively. To generate the conditioned media, we could either use VSVΔ51 G-less, a variant of VSV that cannot bud out of the cell, or infect cells with VSVΔ51 and subsequently filter out the virus using centricon filters with a cut-off smaller than the virus (100kDa). The conditioned media could also be used on normal cells to test our hypothesis that TNFα and IFNβ synergy is sufficient to protect normal cells against infection.

It would also be interesting to assess the effects of the VSes on the adaptive immune response, given that TNFα and IL-6 have important roles in regulating various processes from antigen presenting cell maturation to T-cell activation [153–155]. For example, IL-6 has been shown to inhibit apoptosis and cytotoxic T-Cell-mediated killing of virus-infected cells [156,157]. Therefore, inhibition of IL-6 production by VSe1 and VSe1-28 could potentially enhance the killing of the infected tumour cells by cytotoxic T cells. However, we have yet to determine if VSe1 and VSe1-28 inhibit the production of these cytokines in surrounding normal cells, which also play an important role in regulating the activation and recruitment of immune cells.

4.4 Impact of Cellular GSH Levels on Viral Sensitization

As previously mentioned (section 1.5.3), glutathionylation of NFκB has been reported to inhibit both its nuclear translocation and its DNA-binding activity, and glutathionylation can be induced using small molecules such as cinnamaldehyde [130,132].We demonstrate here that cinnamaldehyde can also enhance OV infection and oncolysis of 786-0 human renal carcinoma cells (**Fig 13**), although at much higher concentrations than those used in the aforementioned study. However, we have yet to assess the effects of cinnamaldehyde on NFκB activity at the concentration we used in our model. Although our results show that VSe1 and VSe1-28 modulate cellular GSH levels similarly to cinnamaldehyde (**Fig 12**), the extent of the GSH depletion and the kinetics slightly differ from one another. Indeed, VSe1-28 depletes cellular GSH more effectively than VSe1, and the depletion lasts for at least 4 hours (**Fig 12**). When NFκB glutathionylation was assessed by immunoprecipitation, we found that neither VSe1 nor VSe1-28 seem to affect glutathionylation of p65 (**Fig 14a**), therefore suggesting that VSe1 and VSe1-28 inhibit NFκB by other means.

To better understand the relevance of GSH depletion in eliciting the viral enhancing effects of VSe1 and VSe1-28, cells were cultured in buthionine sulfoximine (BSO) for 6-10 days to inhibit the synthesis of GSH. Upon confirming that GSH levels were depleted by HPLC (**Fig 14b**), cells were infected with VSVΔ51 and virus output quantified. We found that BSO slightly enhanced virus replication, however to lesser levels when compared to our VSes (data not shown). Furthermore, we assessed the combination of BSO and VSe1 or VSe1-28 on virus output and found that the potency of both VSes increased upon depletion of cellular GSH by BSO (**Fig 14c**). Given the known role of GSH in drug resistance, we propose that GSH blocks the activity of VSe1 and VSe1-28 by binding to and inactivating the compounds. Interestingly, we noticed that the renal

carcinoma cell line 786-0 has relatively high basal levels of GSH. Furthermore, the concentration of VSe1 and VSe1-28 optimal for sensitizing 786-0 cells (60μM VSe1 and 80μM VSe1-28) is 2-3 times higher than the optimal concentration in several other cancer cell lines, including OVCA433 (human ovarian cancer) and CT26wt (murine colon carcinoma). To support our hypothesis that GSH impairs VSe1 and VSe1-28 activity, it would be interesting to assess the levels of GSH in other cell lines to see if they correlate with the active doses of the compounds required to sensitize the cells to infection. Given that cellular GSH impairs VSe1 and VSe1-28 activity, our data demonstrates that depletion of GSH is not involved in the mechanism of action of the VSes, and that cellular GSH may hinder their ability to sensitize cells to OV infection.

4.5 ROS-Mediated Inhibition of NFκB Activity

Aside from their effects on GSH homeostasis, we found that the active VSe1 analogues highly upregulate several genes involved in the redox response (**Fig 15**). The induction of HMOX1 and OSGIN by VSe1 and VSe1-28 is most robust at 8 hours, again matching the kinetics of inhibition of NFκB activity and cytokine production (**Fig 16**). Interestingly, many viruses induce the cellular accumulation of ROS [158,159] and in some cases, increased ROS production was even found to be favorable for virus infection [160]. In line with this, we found VSVΔ51 infection to be enhanced by the addition of exogenous H_2O_2 in 786-0 cells (**Fig 17**), although the toxicity to the cells at those concentrations has yet to be determined. Interestingly, NFκB subunits have been reported to contain redox-sensitive residues in their DNA-binding domains that serve important regulatory functions [140]. Indeed, one report demonstrated that the p50 subunit contains a redox-sensitive cysteine (cys-62) that is highly oxidized in the cytoplasm but reduced in the nucleus and that the reduction of cys-62 was essential for the DNA-binding activity of p50 [161]. In line with this, our data demonstrates that NFκB nuclear translocation and transcriptional activity is inhibited by H_2O_2

in a dose-dependant manner (**Fig 18**). Therefore, it is possible that VSe1 and VSe1-28 inhibit NFκB nuclear translocation through the formation of ROS intermediates that bind redox-sensitive residues on either the p50 or p65 subunit of NFκB to prevent cytokine and ISG expression. Indeed, induction of ROS would also result in the upregulation of ROS-induced genes such as HMOX1 and OSGIN and impact GSH homeostasis as described above.

IFNβ production is also regulated by IRF3 and AP1, however their implication in TNFα and IL-6 induction is not described to date. Interestingly, while we show that H_2O_2 inhibits TNFα and IL-6 production in response to infection in a dose-dependant manner, it inhibits IFNβ production at all tested concentrations (**Fig 18b**). This suggests that H_2O_2 could also interfere with IRF3 or AP1 activity, since even partial inhibition of two or more regulators would reduce the required concentration of H_2O_2 needed to inhibit IFNβ production. Furthermore, H_2O_2 has been shown to inhibit STAT1 phosphorylation in liver cells [162], which demonstrates a broad antagonistic effect of H_2O_2 on antiviral pathways. Our results show that H_2O_2 inhibits IFNβ production at as little as 1 mM, a concentration at which virus output was only slightly enhanced. This indicates that inhibition of IFNβ production alone cannot fully sensitize 786-0 cells to infection. It is tempting to suggest that the combined inhibition of the secretion of IFNβ and TNFα or other factors produced in response to virus infection is required to achieve robust viral sensitization.

4.6 Direct Inhibition of NFκB by VSe1 and VSe1-28

Although our data indicate that VSes might inhibit NFκB through the formation of ROS intermediates, we have not yet ruled out the possibility of the VSes directly binding and inhibiting proper function of NFκB. Since the compounds are variably electrophilic in nature (particularly VSe1), it is possible for them to bind nucleophilic cysteine residues of p50 and/or p65. To test this, new 'clickable' VSe analogues were synthesized with functional groups that support

thermodynamically-favored reactions that lead specifically to one product (a process known as click chemistry). These modified analogues can be used to attach fluorophores or biotin groups to the compound even after a compound has reacted with another target (e.g. a protein). The clickable VSe analogue has been tested *in vitro* and maintains its viral sensitizing ability, albeit at higher concentrations (data not shown). Using these clickable variants, we could treat cells prior to infection with VSVΔ51 and collect lysates, at which point click-chemistry could be used to attach fluorophores to the VSes. p65 or p50 can then be immunoprecipitated and loaded onto a polyacrylamide gel. If the VSes bind either NFκB subunit, we should detect a fluorescent signal at their respective molecular weights. As previously mentioned, biotin can also be conjugated to the clickable VSes. This would allow us to pull down VSes from cell lysates of using streptavidin and mass spectrometry could be used to identify any interacting partner. These experiments would determine if there is a direct interaction between the VSes and NFκB, and also identify other potential targets of our VSes.

5. Conclusion

OV therapy is a promising biotherapeutic approach for the treatment of cancer, however resistance and heterogeneity of tumors hinder its potential. Our group has previously identified and synthesized VSes that sensitize cells to OV infection. In this study, we demonstrate that these VSes are potent inhibitors of NFκB nuclear translocation and transcriptional activity, which in turn inhibits the production of the antiviral cytokines IFNβ, TNFα and IL-6. We also provide evidence supporting the possibility that inhibition of NFκB by the VSes may be a result of the formation of ROS intermediates that that lead to reduced nuclear translocation of NFκB subunits, thereby preventing NFκB-mediated cytokine production.

The results obtained in this study provide important insights for uncovering the specific mechanism of action of our VSes. Furthermore, we demonstrate a novel finding that OV infection of resistant cancer cells can be enhanced through redox-mediated modulation of innate antiviral response. Altogether, the findings of this study contribute to the continued development of combination therapies that synergize with OV-therapy as well as the development of new generations of optimal VSes.

References

1. Canadian Cancer Society. Canadian Cancer Statistics Special Topic: Pancreatic Cancer. (2017).
2. Jackson, S. P. & Bartek, J. The DNA-damage response in human biology and disease. *Nature* **461,** 1071–8 (2009).
3. zur Hausen, H. Papillomaviruses and cancer: from basic studies to clinical application. *Nat. Rev. Cancer* **2,** 342–350 (2002).
4. Hanahan, D. & Weinberg, R. A. Hallmarks of Cancer: The Next Generation. *Cell* **144,** 646–674 (2011).
5. Malhotra, V. & Perry, M. C. Classical chemotherapy: mechanisms, toxicities and the therapeutic window. *Cancer Biol Ther* **2,** S2-4 (2003).
6. Fu, D., Calvo, J. A. & Samson, L. D. Balancing repair and tolerance of DNA damage caused by alkylating agents. *Nat. Rev. Cancer* **12,** 104–20 (2012).
7. Tiwari, M. Antimetabolites: Established cancer therapy. *J. Cancer Res. Ther.* **8,** 510 (2012).
8. Jordan, M. A. & Wilson, L. Microtubules as a target for anticancer drugs. *Nat. Rev. Cancer* **4,** 253–265 (2004).
9. Russell, S. J., Peng, K.-W. & Bell, J. C. Oncolytic virotherapy. *Nat. Biotechnol.* **30,** 658–70 (2012).
10. Russell, S. J. & Peng, K.-W. Viruses as anticancer drugs. *Trends Pharmacol. Sci.* **28,** 326–33 (2007).
11. Ilkow, C. S., Swift, S. L., Bell, J. C. & Diallo, J.-S. From Scourge to Cure: Tumour-Selective Viral Pathogenesis as a New Strategy against Cancer The Tumour: A Unique Niche for Virus Growth. doi:10.1371/journal.ppat.1003836
12. Kelly, E. & Russell, S. J. History of Oncolytic Viruses: Genesis to Genetic Engineering. *Mol. Ther.* **15,** 651–659 (2007).
13. Breitbach, C. J. *et al.* Targeted Inflammation During Oncolytic Virus Therapy Severely Compromises Tumor Blood Flow. *Mol. Ther.* **15,** 1686–1693 (2007).
14. Breitbach, C. J. *et al.* Targeting Tumor Vasculature With an Oncolytic Virus. *Mol. Ther.* **19,** 886–894 (2011).
15. Bridle, B. W. *et al.* Oncolytic vesicular stomatitis virus quantitatively and qualitatively improves primary CD8 $^{+}$ T-cell responses to anticancer vaccines. *Oncoimmunology* **2,** e26013 (2013).
16. Zhang, J. *et al.* Maraba MG1 Virus Enhances Natural Killer Cell Function via Conventional Dendritic Cells to Reduce Postoperative Metastatic Disease. *Mol. Ther.* **22,** 1320–1332 (2014).

17. Workenhe, S. T., Verschoor, M. L. & Mossman, K. L. The role of oncolytic virus immunotherapies to subvert cancer immune evasion. *Futur. Oncol.* **11,** 675–689 (2015).

18. Workenhe, S. T. *et al.* Immunogenic HSV-mediated Oncolysis Shapes the Antitumor Immune Response and Contributes to Therapeutic Efficacy. *Mol. Ther.* **22,** 123–131 (2014).

19. Mccart, J. A. *et al.* Systemic Cancer Therapy with a Tumor-selective Vaccinia Virus Mutant Lacking Thymidine Kinase and Vaccinia Growth Factor Genes. *CANCER Res.* **61,** 8751–8757 (2001).

20. Brun, J. *et al.* Identification of genetically modified Maraba virus as an oncolytic rhabdovirus. *Mol Ther* **18,** 1440–1449 (2010).

21. Zhang, J. *et al.* A novel oncolytic adenovirus targeting Wnt signaling effectively inhibits cancer-stem like cell growth via metastasis, apoptosis and autophagy in HCC models. *Biochem. Biophys. Res. Commun.* **491,** 469–477 (2017).

22. Leveille, S., Samuel, S., Goulet, M.-L. & Hiscott, J. Enhancing VSV oncolytic activity with an improved cytosine deaminase suicide gene strategy. *Cancer Gene Ther.* **18,** 435–443 (2011).

23. Le Boeuf, F. *et al.* Reovirus FAST Protein Enhances Vesicular Stomatitis Virus Oncolytic Virotherapy in Primary and Metastatic Tumor Models. *Mol. Ther. - Oncolytics* **6,** 80–89 (2017).

24. Ben Yebdri, F. *et al.* Triptolide-Mediated Inhibition of Interferon Signaling Enhances Vesicular Stomatitis Virus-Based Oncolysis. *Mol. Ther.* **21,** 2043–2053 (2013).

25. Bourgeois-Daigneault, M.-C. *et al.* Combination of Paclitaxel and MG1 oncolytic virus as a successful strategy for breast cancer treatment. *Breast Cancer Res.* **18,** 83 (2016).

26. Letchworth, G. J., Rodriguez, L. L. & Del cbarrera, J. Vesicular stomatitis. *Vet. J.* **157,** 239–60 (1999).

27. Regan, A. D. & Whittaker, G. R. Entry of rhabdoviruses into animal cells. *Adv. Exp. Med. Biol.* **790,** 167–77 (2013).

28. Finkelshtein, D., Werman, A., Novick, D., Barak, S. & Rubinstein, M. LDL receptor and its family members serve as the cellular receptors for vesicular stomatitis virus. *Proc. Natl. Acad. Sci.* **110,** 7306–7311 (2013).

29. Durrer, P., Gaudin, Y., Ruigrok, R. W., Graf, R. & Brunner, J. Photolabeling identifies a putative fusion domain in the envelope glycoprotein of rabies and vesicular stomatitis viruses. *J. Biol. Chem.* **270,** 17575–81 (1995).

30. Brown, J. C., Newcomb, W. W. & Lawrenz-Smith, S. pH-dependent accumulation of the vesicular stomatitis virus glycoprotein at the ends of intact virions. *Virology* **167,** 625–9 (1988).

31. Puri, A., Krumbiegel, M., Dimitrov, D. & Blumenthal, R. A new approach to measure fusion activity of cloned viral envelope proteins: fluorescence dequenching of

octadecylrhodamine-labeled plasma membrane vesicles fusing with cells expressing vesicular stomatitis virus glycoprotein. *Virology* **195,** 855–8 (1993).

32. Green, T. J. & Luo, M. Structure of the vesicular stomatitis virus nucleocapsid in complex with the nucleocapsid-binding domain of the small polymerase cofactor, P. *Proc. Natl. Acad. Sci. U. S. A.* **106,** 11713–8 (2009).

33. Gao, Y. & Lenard, J. Cooperative binding of multimeric phosphoprotein (P) of vesicular stomatitis virus to polymerase (L) and template: pathways of assembly. *J. Virol.* **69,** 7718–23 (1995).

34. Li, J., Rahmeh, A., Morelli, M. & Whelan, S. P. J. A conserved motif in region v of the large polymerase proteins of nonsegmented negative-sense RNA viruses that is essential for mRNA capping. *J. Virol.* **82,** 775–84 (2008).

35. Li, J., Fontaine-Rodriguez, E. C. & Whelan, S. P. J. Amino acid residues within conserved domain VI of the vesicular stomatitis virus large polymerase protein essential for mRNA cap methyltransferase activity. *J. Virol.* **79,** 13373–84 (2005).

36. Ogino, T. & Banerjee, A. K. Unconventional Mechanism of mRNA Capping by the RNA-Dependent RNA Polymerase of Vesicular Stomatitis Virus. *Mol. Cell* **25,** 85–97 (2007).

37. Grdzelishvili, V. Z. *et al.* A Single Amino Acid Change in the L-Polymerase Protein of Vesicular Stomatitis Virus Completely Abolishes Viral mRNA Cap Methylation. *J. Virol.* **79,** 7327–7337 (2005).

38. Grdzelishvili, V. Z. *et al.* Identification of a new region in the vesicular stomatitis virus L polymerase protein which is essential for mRNA cap methylation. *Virology* **350,** 394–405 (2006).

39. Emerson, S. U. & Wagner, R. R. L protein requirement for in vitro RNA synthesis by vesicular stomatitis virus. *J. Virol.* **12,** 1325–35 (1973).

40. Redondo, N. *et al.* Impact of Vesicular Stomatitis Virus M Proteins on Different Cellular Functions. *PLoS One* **10,** e0131137 (2015).

41. von Kobbe C *et al.* Vesicular stomatitis virus matrix protein inhibits host cell gene expression by targeting the nucleoporin Nup98. *Mol. Cell* **6,** 1243–52 (2000).

42. Her, L. S., Lund, E. & Dahlberg, J. E. Inhibition of Ran guanosine triphosphatase-dependent nuclear transport by the matrix protein of vesicular stomatitis virus. *Science* **276,** 1845–8 (1997).

43. Rajani, K. R. *et al.* Complexes of vesicular stomatitis virus matrix protein with host Rae1 and Nup98 involved in inhibition of host transcription. *PLoS Pathog.* **8,** e1002929 (2012).

44. Connor, J. H. & Lyles, D. S. Vesicular stomatitis virus infection alters the eIF4F translation initiation complex and causes dephosphorylation of the eIF4E binding protein 4E-BP1. *J. Virol.* **76,** 10177–87 (2002).

45. Black, B. L., Brewer, G. & Lyles, D. S. Effect of vesicular stomatitis virus matrix protein on host-directed translation in vivo. *J. Virol.* **68,** 555–60 (1994).

46. Lichty, B. D., Power, A. T., Stojdl, D. F. & Bell, J. C. Vesicular stomatitis virus: re-inventing the bullet. *Trends Mol. Med.* **10,** 210–216 (2004).

47. Stojdl, D. F. *et al.* VSV strains with defects in their ability to shutdown innate immunity are potent systemic anti-cancer agents. *Cancer Cell* **4,** 263–275 (2003).

48. Takaoka, A. & Yanai, H. Interferon signalling network in innate defence. *Cell. Microbiol.* **8,** 907–922 (2006).

49. Honda, K., Takaoka, A. & Taniguchi, T. Type I Inteferon Gene Induction by the Interferon Regulatory Factor Family of Transcription Factors. *Immunity* **25,** 349–360 (2006).

50. Katze, M. G., Fornek, J. L., Palermo, R. E., Walters, K.-A. & Korth, M. J. Innate immune modulation by RNA viruses: emerging insights from functional genomics. *Nat. Rev. Immunol.* **8,** 644–654 (2008).

51. Kato, H. *et al.* Differential roles of MDA5 and RIG-I helicases in the recognition of RNA viruses. *Nature* **441,** 101–105 (2006).

52. Jensen, S. & Thomsen, A. R. Sensing of RNA Viruses: a Review of Innate Immune Receptors Involved in Recognizing RNA Virus Invasion. doi:10.1128/JVI.05738-11

53. Rassa, J. C., Meyers, J. L., Zhang, Y., Kudaravalli, R. & Ross, S. R. Murine retroviruses activate B cells via interaction with toll-like receptor 4. *Proc. Natl. Acad. Sci. U. S. A.* **99,** 2281–6 (2002).

54. Thompson, M. R., Kaminski, J. J., Kurt-Jones, E. A. & Fitzgerald, K. A. Pattern recognition receptors and the innate immune response to viral infection. *Viruses* **3,** 920–40 (2011).

55. Kurt-Jones, E. A. *et al.* Pattern recognition receptors TLR4 and CD14 mediate response to respiratory syncytial virus. *Nat. Immunol.* **1,** 398–401 (2000).

56. Georgel, P. *et al.* Vesicular stomatitis virus glycoprotein G activates a specific antiviral Toll-like receptor 4-dependent pathway. *Virology* **362,** 304–13 (2007).

57. Lund, J. M. *et al.* Recognition of single-stranded RNA viruses by Toll-like receptor 7. *Proc. Natl. Acad. Sci. U. S. A.* **101,** 5598–603 (2004).

58. Kane, M. *et al.* Innate immune sensing of retroviral infection via Toll-like receptor 7 occurs upon viral entry. *Immunity* **35,** 135–45 (2011).

59. Diebold, S. S., Kaisho, T., Hemmi, H., Akira, S. & Reis e Sousa, C. Innate antiviral responses by means of TLR7-mediated recognition of single-stranded RNA. *Science* **303,** 1529–31 (2004).

60. Heil, F. *et al.* Species-specific recognition of single-stranded RNA via toll-like receptor 7 and 8. *Science* **303,** 1526–9 (2004).

61. Medzhitov, R. *et al.* MyD88 is an adaptor protein in the hToll/IL-1 receptor family signaling pathways. *Mol. Cell* **2,** 253–8 (1998).

62. Moynagh, P. N. TLR signalling and activation of IRFs: revisiting old friends from the NF-κB pathway. *Trends Immunol.* **26,** 469–476 (2005).

63. Sharma, S. *et al.* Triggering the Interferon Antiviral Response Through an IKK-Related Pathway. *Science (80-.).* **300,** 1148–1151 (2003).

64. Fitzgerald, K. A. *et al.* IKKε and TBK1 are essential components of the IRF3 signaling pathway. *Nat. Immunol.* **4,** 491–496 (2003).

65. Suhara, W. *et al.* Analyses of virus-induced homomeric and heteromeric protein associations between IRF-3 and coactivator CBP/p300. *J. Biochem.* **128,** 301–7 (2000).

66. Yoneyama, M. *et al.* Direct triggering of the type I interferon system by virus infection: activation of a transcription factor complex containing IRF-3 and CBP/p300. *EMBO J.* **17,** 1087–95 (1998).

67. Lin, R., Heylbroeck, C., Pitha, P. M. & Hiscott, J. Virus-dependent phosphorylation of the IRF-3 transcription factor regulates nuclear translocation, transactivation potential, and proteasome-mediated degradation. *Mol. Cell. Biol.* **18,** 2986–96 (1998).

68. Weaver, B. K., Kumar, K. P. & Reich, N. C. Interferon regulatory factor 3 and CREB-binding protein/p300 are subunits of double-stranded RNA-activated transcription factor DRAF1. *Mol. Cell. Biol.* **18,** 1359–68 (1998).

69. Honda, K. & Taniguchi, T. IRFs: master regulators of signalling by Toll-like receptors and cytosolic pattern-recognition receptors. *Nat. Rev. Immunol.* **6,** 644–658 (2006).

70. Platanias, L. C. Mechanisms of type-I- and type-II-interferon-mediated signalling. *Nat. Rev. Immunol.* **5,** 375–386 (2005).

71. Huang, Y. *et al.* MAVS-MKK7-JNK2 Defines a Novel Apoptotic Signaling Pathway during Viral Infection. *PLoS Pathog.* **10,** e1004020 (2014).

72. Iordanov, M. S. *et al.* Activation of p38 Mitogen-Activated Protein Kinase and c-Jun NH 2 -Terminal Kinase by Double-Stranded RNA and Encephalomyocarditis Virus: Involvement of RNase L, Protein Kinase R, and Alternative Pathways. **20,** 617–627 (2000).

73. Rincón, M. & Davis, R. J. Regulation of the immune response by stress-activated protein kinases. *Immunol. Rev.* **228,** 212–224 (2009).

74. Eferl, R. & Wagner, E. F. AP-1: a double-edged sword in tumorigenesis. *Nat. Rev. Cancer* **3,** 859–868 (2003).

75. Hoesel, B. & Schmid, J. A. The complexity of NF-κB signaling in inflammation and cancer. *Mol. Cancer* **12,** 1 (2013).

76. Hatakeyama, S. *et al.* Ubiquitin-dependent degradation of IkappaBalpha is mediated by a ubiquitin ligase Skp1/Cul 1/F-box protein FWD1. *Proc. Natl. Acad. Sci. U. S. A.* **96,** 3859–63 (1999).

77. Yaron, A. *et al.* Identification of the receptor component of the IkappaBalpha-ubiquitin ligase. *Nature* **396,** 590–4 (1998).

78. Zhou, A., Scoggin, S., Gaynor, R. B. & Williams, N. S. Identification of NF-jB-regulated genes induced by TNFa utilizing expression profiling and RNA interference. *Oncogene* **22,** 2034–2044 (2003).

79. Sun, S.-C. Non-canonical NF-κB signaling pathway. *Cell Res.* **21,** 71–85 (2011).

80. Solan, N. J., Miyoshi, H., Carmona, E. M., Bren, G. D. & Paya, C. V. RelB cellular regulation and transcriptional activity are regulated by p100. *J. Biol. Chem.* **277,** 1405–18 (2002).

81. Nowak, D. E. *et al.* RelA Ser276 Phosphorylation Is Required for Activation of a Subset of NF- B-Dependent Genes by Recruiting Cyclin-Dependent Kinase 9/Cyclin T1 Complexes. *Mol. Cell. Biol.* **28,** 3623–3638 (2008).

82. Zhong, H., Voll, R. E. & Ghosh, S. Phosphorylation of NF-kappa B p65 by PKA stimulates transcriptional activity by promoting a novel bivalent interaction with the coactivator CBP/p300. *Mol. Cell* **1,** 661–71 (1998).

83. Tago, K., Funakoshi-Tago, M., Sakinawa, M., Mizuno, N. & Itoh, H. κB-Ras Is a Nuclear-Cytoplasmic Small GTPase That Inhibits NF-κB Activation through the Suppression of Transcriptional Activation of p65/RelA. *J. Biol. Chem.* **285,** 30622–30633 (2010).

84. Huang, B., Yang, X.-D., Lamb, A. & Chen, L.-F. Posttranslational modifications of NF-kappaB: another layer of regulation for NF-kappaB signaling pathway. *Cell. Signal.* **22,** 1282–90 (2010).

85. Rothgiesser, K. M., Fey, M. & Hottiger, M. O. Acetylation of p65 at lysine 314 is important for late NF-kappaB-dependent gene expression. *BMC Genomics* **11,** 22 (2010).

86. Pejanovic, N. *et al.* Regulation of Nuclear Factor κB (NF-κB) Transcriptional Activity via p65 Acetylation by the Chaperonin Containing TCP1 (CCT). *PLoS One* **7,** e42020 (2012).

87. Ishinaga, H. *et al.* TGF-β induces p65 acetylation to enhance bacteria-induced NF-κB activation. *EMBO J.* **26,** 1150–1162 (2007).

88. Perkins, N. D. Cysteine 38 Holds the Key to NF-κB Activation. *Mol. Cell* **45,** 1–3 (2012).

89. Sen, N. *et al.* Hydrogen Sulfide-Linked Sulfhydration of NF-κB Mediates Its Antiapoptotic Actions. *Mol. Cell* **45,** 13–24 (2012).

90. Silvennoinen, O., Ihle, J. N., Schlessinger, J. & Levy, D. E. Interferon-induced nuclear signalling by Jak protein tyrosine kinases. *Nature* **366,** 583–5 (1993).

91. Liu, Z. *et al.* The Interferon-Inducible MxB Protein Inhibits HIV-1 Infection. *Cell Host Microbe* **14,** 398–410 (2013).

92. Anafu, A. A., Bowen, C. H., Chin, C. R., Brass, A. L. & Holm, G. H. Interferon-inducible Transmembrane Protein 3 (IFITM3) Restricts Reovirus Cell Entry. *J. Biol. Chem.* **288,** 17261–17271 (2013).

93. Liu, S.-Y. *et al.* Interferon-Inducible Cholesterol-25-Hydroxylase Broadly Inhibits Viral Entry by Production of 25-Hydroxycholesterol. *Immunity* **38,** 92–105 (2013).

94. Liu, S.-Y. *et al.* Interferon-inducible cholesterol-25-hydroxylase broadly inhibits viral entry by production of 25-hydroxycholesterol. *Immunity* **38,** 92–105 (2013).

95. Metz, P. *et al.* Identification of type I and type II interferon-induced effectors controlling hepatitis C virus replication. *Hepatology* **56,** 2082–93 (2012).

96. Wang, S. *et al.* Viperin inhibits hepatitis C virus replication by interfering with binding of NS5A to host protein hVAP-33. *J. Gen. Virol.* **93,** 83–92 (2012).

97. Helbig, K. J. *et al.* The antiviral protein viperin inhibits hepatitis C virus replication via interaction with nonstructural protein 5A. *Hepatology* **54,** 1506–17 (2011).

98. Schneider, W. M., Chevillotte, D. & Rice, C. M. Interferon-Stimulated Genes: A Complex Web of Host Defenses. doi:10.1146/annurev-immunol-032713-120231

99. Goujon, C. *et al.* Human MX2 is an interferon-induced post-entry inhibitor of HIV-1 infection. *Nature* **502,** 559–62 (2013).

100. Kane, M. *et al.* MX2 is an interferon-induced inhibitor of HIV-1 infection. *Nature* **502,** 563–6 (2013).

101. Wilkins, C. *et al.* IFITM1 is a tight junction protein that inhibits hepatitis C virus entry. *Hepatology* **57,** 461–469 (2013).

102. Huang, I.-C. *et al.* Distinct patterns of IFITM-mediated restriction of filoviruses, SARS coronavirus, and influenza A virus. *PLoS Pathog.* **7,** e1001258 (2011).

103. Cheng, P.-H. *et al.* Virotherapy targeting cyclin E overexpression in tumors with adenovirus-enhanced cancer-selective promoter. *J. Mol. Med.* **93,** 211–223 (2015).

104. Le Boeuf, F. *et al.* Synergistic Interaction Between Oncolytic Viruses Augments Tumor Killing. *Mol. Ther.* **18,** 888–895 (2010).

105. Nguyên, T. L.-A. *et al.* Chemical targeting of the innate antiviral response by histone deacetylase inhibitors renders refractory cancers sensitive to viral oncolysis. *Proc. Natl. Acad. Sci. U. S. A.* **105,** 14981–6 (2008).

106. Arulanandam, R. *et al.* Microtubule disruption synergizes with oncolytic virotherapy by inhibiting interferon translation and potentiating bystander killing. *Nat. Commun.* **6,** 1–14 (2015).

107. Diallo, J. S. *et al.* A high-throughput pharmacoviral approach identifies novel oncolytic virus sensitizers. *Mol Ther* **18,** 1123–1129 (2010).

108. Dornan, M. H. *et al.* First-in-class small molecule potentiators of cancer virotherapy. *Sci. Rep.* **6,** 26786 (2016).

109. Lushchak, V. I. Glutathione Homeostasis and Functions: Potential Targets for Medical Interventions. *J. Amino Acids* **736837,** (2012).

110. Sobhakumari, A. *et al.* Susceptibility of Human Head and Neck Cancer Cells to Combined Inhibition of Glutathione and Thioredoxin Metabolism. *PLoS One* **7,** e48175 (2012).

111. Klauser, E., Gülden, M., Maser, E., Seibert, S. & Seibert, H. Additivity, antagonism, and

synergy in arsenic trioxide-induced growth inhibition of C6 glioma cells: Effects of genistein, quercetin and buthionine-sulfoximine. *Food Chem. Toxicol.* **67,** 212–221 (2014).

112. Rodman, S. N. *et al.* Enhancement of Radiation Response in Breast Cancer Stem Cells by Inhibition of Thioredoxin- and Glutathione-Dependent Metabolism. *Radiat. Res.* **186,** 385–395 (2016).

113. Laborde, E. Glutathione transferases as mediators of signaling pathways involved in cell proliferation and cell death. *Cell Death Differ.* **1780,** 1373–1380 (2010).

114. Tew, K. D. *et al.* The Role of Glutathione S-transferase P in signaling pathways and S-glutathionylation in Cancer. doi:10.1016/j.freeradbiomed.2011.04.013

115. Townsend, D. M. *et al.* A glutathione S-transferase pi-activated prodrug causes kinase activation concurrent with S-glutathionylation of proteins. *Mol. Pharmacol.* **69,** 501–8 (2006).

116. Adler, V. *et al.* Regulation of JNK signaling by GSTp. *EMBO J.* **18,** 1321–34 (1999).

117. Pastore, A. & Piemonte, F. *S-Glutathionylation signaling in cell biology: Progress and prospects*. *European Journal of Pharmaceutical Sciences* **46,** 279–292 (2012).

118. Velu, C. S., Niture, S. K., Doneanu, C. E., Pattabiraman, N. & Srivenugopal, K. S. Human p53 is inhibited by glutathionylation of cysteines present in the proximal DNA-binding domain during oxidative stress. *Biochemistry* **46,** 7765–80 (2007).

119. Klatt, P. *et al.* Redox regulation of c-Jun DNA binding by reversible S-glutathiolation. *FASEB J.* **13,** 1481–90 (1999).

120. Prinarakis, E., Chantzoura, E., Thanos, D. & Spyrou, G. S-glutathionylation of IRF3 regulates IRF3-CBP interaction and activation of the IFN beta pathway. *EMBO J.* **27,** 865–875 (2008).

121. Huang, Z., Pinto, J. T., Deng, H. & Richie, J. P. Inhibition of caspase-3 activity and activation by protein glutathionylation. *Biochem. Pharmacol.* **75,** 2234–44 (2008).

122. Anathy, V. *et al.* Redox amplification of apoptosis by caspase-dependent cleavage of glutaredoxin 1 and S-glutathionylation of Fas. *J. Cell Biol.* **184,** 241–52 (2009).

123. Fratelli, M. *et al.* Identification by redox proteomics of glutathionylated proteins in oxidatively stressed human T lymphocytes. *Proc. Natl. Acad. Sci. U. S. A.* **99,** 3505–10 (2002).

124. Passarelli, C., Tozzi, G., Pastore, A., Bertini, E. & Piemonte, F. GSSG-mediated Complex I defect in isolated cardiac mitochondria. *Int. J. Mol. Med.* **26,** 95–9 (2010).

125. Chen, Y.-R., Chen, C.-L., Pfeiffer, D. R. & Zweier, J. L. Mitochondrial complex II in the post-ischemic heart: oxidative injury and the role of protein S-glutathionylation. *J. Biol. Chem.* **282,** 32640–54 (2007).

126. Garcia, J. *et al.* Regulation of mitochondrial glutathione redox status and protein glutathionylation by respiratory substrates. *J. Biol. Chem.* **285,** 39646–54 (2010).

127. Reynaert, N. L. *et al.* Dynamic redox control of NF-kappaB through glutaredoxin-regulated S-glutathionylation of inhibitory kappaB kinase beta. *Proc. Natl. Acad. Sci. U. S. A.* **103,** 13086–91 (2006).

128. Kil, I. S., Kim, S. Y. & Park, J.-W. Glutathionylation regulates IkappaB. *Biochem. Biophys. Res. Commun.* **373,** 169–73 (2008).

129. Pineda-Molina, E. *et al.* Glutathionylation of the p50 subunit of NF-kappaB: a mechanism for redox-induced inhibition of DNA binding. *Biochemistry* **40,** 14134–42 (2001).

130. Liao, B.-C., Hsieh, C.-W., Lin, Y.-C. & Wung, B.-S. The Glutaredoxin/Glutathione System Modulates NF-κB Activity by Glutathionylation of p65 in Cinnamaldehyde-Treated Endothelial Cells. *Toxicol. Sci.* **116,** 151–163 (2010).

131. Qanungo, S. *et al.* N-acetyl-l-cysteine sensitizes pancreatic cancers to gemcitabine by targeting the NFκB pathway. *Biomed. Pharmacother.* **68,** 855–864 (2014).

132. Qanungo, S., Starke, D. W., Pai, H. V, Mieyal, J. J. & Nieminen, A.-L. Glutathione supplementation potentiates hypoxic apoptosis by S-glutathionylation of p65-NFkappaB. *J. Biol. Chem.* **282,** 18427–36 (2007).

133. Diallo, J. S., Vaha-Koskela, M., Le Boeuf, F. & Bell, J. Propagation, purification, and in vivo testing of oncolytic vesicular stomatitis virus strains. *Methods Mol Biol* **797,** 127–140 (2012).

134. Garcia, V. *et al.* High-throughput titration of luciferase-expressing recombinant viruses. *J. Vis. Exp.* 51890 (2014). doi:10.3791/51890

135. Vultur, A. *et al.* Cell-to-cell adhesion modulates Stat3 activity in normal and breast carcinoma cells. *Oncogene* **23,** 2600–16 (2004).

136. Pfaffl, M. W. A new mathematical model for relative quantification in real-time RT-PCR. *Nucleic Acids Res.* **29,** e45 (2001).

137. Eden, E., Navon, R., Steinfeld, I., Lipson, D. & Yakhini, Z. GOrilla: a tool for discovery and visualization of enriched GO terms in ranked gene lists. *BMC Bioinformatics* **10,** 48 (2009).

138. Mailloux, R. J. *et al.* Glutaredoxin-2 is required to control oxidative phosphorylation in cardiac muscle by mediating deglutathionylation reactions. *J. Biol. Chem.* **289,** 14812–28 (2014).

139. Pierce, J. W. *et al.* Novel inhibitors of cytokine-induced IkappaBalpha phosphorylation and endothelial cell adhesion molecule expression show anti-inflammatory effects in vivo. *J. Biol. Chem.* **272,** 21096–103 (1997).

140. Kabe, Y., Ando, K., Hirao, S., Yoshida, M. & Handa, H. Redox Regulation of NF-κB Activation: Distinct Redox Regulation Between the Cytoplasm and the Nucleus. *Antioxid. Redox Signal.* **7,** 395–403 (2005).

141. Paglino, J. C. & van den Pol, A. N. Vesicular stomatitis virus has extensive oncolytic activity against human sarcomas: rare resistance is overcome by blocking interferon

pathways. *J. Virol.* **85,** 9346–58 (2011).

142. Escobar-Zarate, D., Liu, Y.-P., Suksanpaisan, L., Russell, S. J. & Peng, K.-W. Overcoming cancer cell resistance to VSV oncolysis with JAK1/2 inhibitors. *Cancer Gene Ther.* **20,** 582–9 (2013).

143. Pfeffer, L. M. The Role of Nuclear Factor kB in the Interferon Response. doi:10.1089/jir.2011.0028

144. Hoesel, B. & Schmid, J. A. The complexity of NF-κB signaling in inflammation and cancer. *Mol. Cancer* **12,** 86 (2013).

145. Gupta, S. C., Sundaram, C., Reuter, S. & Aggarwal, B. B. Inhibiting NF-κB activation by small molecules as a therapeutic strategy. *Biochim. Biophys. Acta* **1799,** 775–87 (2010).

146. Gagné, B., Tremblay, N., Park, A. Y., Baril, M. & Lamarre, D. Importin β1 targeting by hepatitis C virus NS3/4A protein restricts IRF3 and NF-κB signaling of IFNB1 antiviral response. *Traffic* **18,** 362–377 (2017).

147. Baud, V. & Collares, D. Post-Translational Modifications of RelB NF-κB Subunit and Associated Functions. doi:10.3390/cells5020022

148. Perkins, N. Post-translational modifications regulating the activity and function of the nuclear factor kappa B pathway. *Oncogene* **25,** 6717–6730 (2006).

149. Leidner, J. *et al.* SUMOylation Attenuates the Transcriptional Activity of the NF-κB Subunit RelB. *J. Cell. Biochem.* **115,** 1430–1440 (2014).

150. Hu, J. & Colburn, N. H. Histone Deacetylase Inhibition Down-Regulates Cyclin D1 Transcription by Inhibiting Nuclear Factor- B/p65 DNA Binding. *Mol. Cancer Res.* **3,** 100–109 (2005).

151. Deng, W.-G., Tang, S.-T., Tseng, H.-P. & Wu, K. K. Melatonin suppresses macrophage cyclooxygenase-2 and inducible nitric oxide synthase expression by inhibiting p52 acetylation and binding. *Blood* **108,** 518–524 (2006).

152. Bartee, E., Mohamed, M. R., Lopez, M. C., Baker, H. V. & McFadden, G. The Addition of Tumor Necrosis Factor plus Beta Interferon Induces a Novel Synergistic Antiviral State against Poxviruses in Primary Human Fibroblasts. *J. Virol.* **83,** 498–511 (2009).

153. Scheller, J., Chalaris, A., Schmidt-Arras, D. & Rose-John, S. The pro- and anti-inflammatory properties of the cytokine interleukin-6. *Biochim. Biophys. Acta - Mol. Cell Res.* **1813,** 878–888 (2011).

154. Zou, G. M. & Tam, Y. K. Cytokines in the generation and maturation of dendritic cells: recent advances. *Eur. Cytokine Netw.* **13,** 186–99

155. Kuhweide, R., van Damme, J. & Ceuppens, J. L. Tumor necrosis factor-α and interleukin 6 synergistically induce T cell growth. *Eur. J. Immunol.* **20,** 1019–1025 (1990).

156. Hou, W., Jin, Y.-H., Kang, H. S. & Kim, B. S. Interleukin-6 (IL-6) and IL-17 synergistically promote viral persistence by inhibiting cellular apoptosis and cytotoxic T cell function. *J. Virol.* **88,** 8479–89 (2014).

157. Wu, W. *et al.* TLR ligand induced IL-6 counter- regulates the anti-viral CD8 T cell response during an acute retrovirus infection. (2015). doi:10.1038/srep10501

158. Ma, Q. *et al.* A role for virally induced reactive oxygen species in Kaposi's sarcoma herpesvirus tumorigenesis. *Antioxid. Redox Signal.* **18,** 80–90 (2013).

159. Teoh, M. L. T., Turner, P. V & Evans, D. H. Tumorigenic poxviruses up-regulate intracellular superoxide to inhibit apoptosis and promote cell proliferation. *J. Virol.* **79,** 5799–811 (2005).

160. Ivanov, A. V, Bartosch, B., Smirnova, O. A., Isaguliants, M. G. & Kochetkov, S. N. HCV and oxidative stress in the liver. *Viruses* **5,** 439–69 (2013).

161. Nishi, T. *et al.* Spatial redox regulation of a critical cysteine residue of NF-kappa B in vivo. *J. Biol. Chem.* **277,** 44548–56 (2002).

162. Di Bona, D. *et al.* Oxidative stress inhibits IFN-alpha-induced antiviral gene expression by blocking the JAK-STAT pathway. *J. Hepatol.* **45,** 271–9 (2006).

Contribution from Collaborators

Ramya Krishnan generated the data shown in figure 11 and figure 14 c.

David Patten from Dr. Mary-Ellen Harper's lab assisted with measuring GSH and GSSG levels by HPLC.

Mohammed Selman analyzed the microarray data.

Dr. Christopher Boddy's lab synthesizes all the viral sensitizers.

Curriculum Vitae

Education

University of Ottawa
2015-2017
Biochemistry MSc
Supervisor: Dr. Jean-Simon Diallo
Co-supervisor: Dr. Christopher Boddy

University of Ottawa
2011-2015
Bachelor of Science
Honours Biopharmaceutical Science, Medicinal Chemistry Specialization

Laboratory and Research Experience

Master's Project
2015-2017
Dr. Jean-Simon Diallo – University of Ottawa/OHRI
Small molecule enhancers of oncolytic virotherapy suppress innate antiviral response

- We have demonstrated that our viral sensitizers suppress the antiviral response by inhibiting NFκB activity. Our hypothesis is that our compounds modulate post-translational modifications that hinder NFκB activity.

Honours Project
2014-2015
Dr. Jean-Simon Diallo – University of Ottawa/OHRI
Small molecule enhancers of oncolytic virotherapy suppress innate antiviral response

- We have demonstrated that our viral sensitizers inhibit the transcription of many interferon-stimulated genes and block the response to, and expression of type-I IFNs.

Summer Student
May-Sep 2014
Dr. Jean-Simon Diallo – University of Ottawa/OHRI
Ex vivo analysis of viral sensitizers in order to identify potent compounds for SAR development.

- We have tested several structural analogues of our viral sensitizer, VSe1, *in vitro* and *ex vivo* and identified a lead compound that has improved physiochemical properties while retaining activity and selectivity as a viral sensitizer.

Teaching Experience

Honours Project Supervisor
2016-2017
Supervising the senior research project of an undergraduate student

- Characterizing the effect of ROS on the innate antiviral response and VSV infection.

Teaching Assistant – General Chemistry Laboratory
Fall Semester (2015-2016)

Publications

First-in-class small molecule potentiators of cancer virotherapy
Scientific Reports, May 2016
Dornan MH, Krishnan R, Macklin AM, Selman M, **El Sayes N**, Son HH, Davis C, Chen A, Keillor K, Le PJ, Moi C, Ou P, Pardin C, Canez CR, Le Boeuf F, Bell JC, Smith JC, Diallo JS and Boddy CN

Multi-Modal Potentiation of Oncolytic Virotherapy by Vanadium Compounds
Molecular Therapy, Jan 2018
Mohammed Selman, Christopher Rousso, Anabel Bergeron, Hwan Hee Son, Ramya Krishnan, **Nader A. El-Sayes**, Oliver Varette, Andrew Chen, Fanny Tzelepis, John C. Bell, Debbie Crans, Jean-Simon Diallo

Neo-Adjuvant Oncolytic Virotherapy Prior to Surgery Sensitizes Triple-Negative Breast Cancer to Immune Checkpoint Therapy
Science Translational Medicine, Jan 2018
M.-C. Bourgeois-Daigneault, D. G. Roy*, A. S. Aitken*, **N. A. El Sayes***, T. Falls, O. Varette, L. E. St-Germain, N. Martin, A. Pelin, J.-S. Diallo, B. D. Lichty, D. F. Stojdl, G. Ungerechts, J. C. Bell

Glutathione Imbalance Sensitizes Cancer Cells to Viral Infection via NF-kappaB
To be Submitted
Ramya Krishnan*, **Nader El Sayes***, Johanne Mathieu, Mohammed Selman, Andrew Macklin, Mark Dornan, Hilary Groom, David Patten, Colin Davis, Frances Lai, Brian Lichty, Mary-Ellen Harper, Rozanne Arulanandam, John C. Bell, Tommy Alain, David Josephy, Jeffrey C. Smith, Christopher N. Boddy, Jean-Simon Diallo.

* Equal contribution

Presentations and Conferences

BMI Seminar Day
March 2017
Oral Presentation

OHRI Research Day
Nov 2016
Poster Presentation

International Meeting on Replicating Oncolytic Virus Therapeutics
Oct 2016
Poster Presentation

Summit for Cancer Immunotherapy
June 2016
Poster Presentation

BMI Poster Day
May 2016
Poster Presentation

OHRI Research Day
Nov 2015
Poster Presentation

Volunteer Experience

2014-2017 Fundraising team for the Terry Fox Foundation for cancer research

2014-2017 Worked with the Syrian Association of Ottawa in assisting refugees to integrate into Canadian society

2012-2014 Science Student Association at University of Ottawa

2010 Model United Nations ambassador